THE TECTONICS AND GEOMORPHOLOGY OF THE MOMA RANGE, NE RUSSIA

By

Benjamin G. Johnson

A THESIS

Submitted to
Michigan State University
in partial fulfillment of the requirements
for the degree of

Geological Sciences – Master of Science

2013

ABSTRACT

TECTONICS AND GEOMORPHOLOGY OF THE MOMA RANGE, NE RUSSIA

By

Benjamin G. Johnson

The Moma Range is a Late Cretaceous to Cenozoic, northeast verging fold-and-thrust belt situated along the western boundary of the North American plate in northeast Asia. The slow convergence between North America, Eurasia, and Okhotsk results in a zone of diffuse continental deformation. While the Moma Range is >150 km northeast of main plate boundary zone, the geomorphic character of major rivers along its northeast slope and the recent large-magnitude (up to 6.6 M_{ww}) teleseismic earthquakes indicate that the Moma Range is actively undergoing crustal shortening and accommodating regional convergence.

Changes in channel morphology, river knickpoints, and steepened channels suggest the existence of a break in uplift rates along a previously mapped thrust-sense shear zone. In the central portions of the fold-and-thrust, the deformation is focused along a structure ~30 km inboard of the deformation front. However, the large-magnitude earthquakes are focused in the western portions of the Moma Range, along thrust faults closer to outer edge of the fold-and-thrust belt. These contrasting styles of deformation along-strike are potentially linked to variations in decollement strength, syntectonic sedimentation, and the middle Cenozoic rifting event that shut down convergence in region. This brief rifting event may have caused significant thinning of the orogenic wedge of the fold-an-thrust belt by means of erosion and possibly crustal thinning. By the Pliocene, the North American-–Eurasian rotation pole shifted north of The Moma Range, reestablishing convergence in the region, and resulting in the continued growth and internal deformation of the fold-and-thrust belt.

ACKNOWLEDGEMENTS

Foremost, I would to like to acknowledge the endless help and intellectual guidance of my advisor, Kaz Fujita, without him this project would have never gotten off the ground, nor reached its completion. He introduced me to plate tectonics and showed me what it takes to be scientist. Most importantly, Kaz believed in me, often at times when not many did, and for that I will always be indebted to him

I would also like to extend my gratitude to my other committee members, Kevin Mackey and Brian Hampton: Kevin for his wealth of knowledge on all things Russian; and Brian for helping me develop as a geologist, and for showing me the bigger picture.

Michigan State was a wonderful place for a geology graduate student. Professors like Tyrone Rooney, Grahame Larsen, and Alan Arbogast, got me outside, away from the computer, where geology is truly learned. Andrew Cyr (a guest lecturer) introduced me to the stream profiler and ArcGIS methods. Renate Snider helped with the early stages writing, and Dan Burke helped get things polished near the end. And I'm pretty sure I learned a great deal more from all the students I TAed then they ever learned from me.

Without the companionship of my closest friends and family, my motivation to finish would have long expired. Patricia was endless with her patients during the late nights and weekends of writing. Blaze Budd, Matt Malkowski, Carl Fraser, and Brian Sparks were always there when I needed beer. My siblings, Sam, Ashley and Kyle, let me forget about the stresses graduate life over holiday breaks and vacations to Colorado. Lastly, I need to thank my parents, Jim and Barb Johnson, whose selfless love and support kept me a-float when times were hard.

TABLE OF CONTENTS

LIST OF FIGURES

1. INTRODUCTION

The original plate tectonic paradigm divides the Earth's lithosphere into rigid plates, and requires that all motion between the rigid plates occur at their boundaries (e.g., Morgan, 1968). However, within continent-continent collisional and accretionary orogens, plate boundaries are commonly characterized by zones of diffuse deformation (e.g., England and Jackson, 1989; Gordon, 1995, 1998; Bird, 2003; Cawood et al., 2009). Among these complex intracontinental settings is the Verkhoyansk—Kolyma orogen (VKO), a broad mountain belt of diffuse deformation presently situated within the boundary region of the North American, Eurasian, and Okhotsk plates in northeast Asia (Fig. 1).

The VKO extends from the Lena River in the west to the Kolyma River in the east (Fig. 1), covering an area of nearly 2 million km^2. The region is sparsely populated, generally inaccessible, and home to the coldest temperatures in the northern hemisphere. Adding to these logistical issues; Soviet control for much of the 20^{th} century kept western scientists from entering the region until the late 1980's, and very little of the original Soviet geologic literature has been readily available, let alone translated into English. These issues have confined western study of the region mostly to seismological studies (e.g., Chapman and Solomon, 1976; Cook et al., 1986; Riegel et al., 1993; Mackey et al., 1998; Fujita et al., 2009), a few geodetic investigations (Calais et al., 2003; DeMets et al., 1990; Gaina et al., 2002; Merkouriev and DeMets, 2008), and one geochronology study (Layer et al., 2001); all of which are primarily focused on delineating the main tectonic boundaries within the VKO. These tectonic boundaries are traditionally drawn along the major, seismically active, strike-slip faults that traverse the VKO's interior (Fig. 1); however, the entire region is enclosed by the two, outward verging, fold-and-thrust belts, the Verkhoyansk and the Moma Range (Fig. 1).

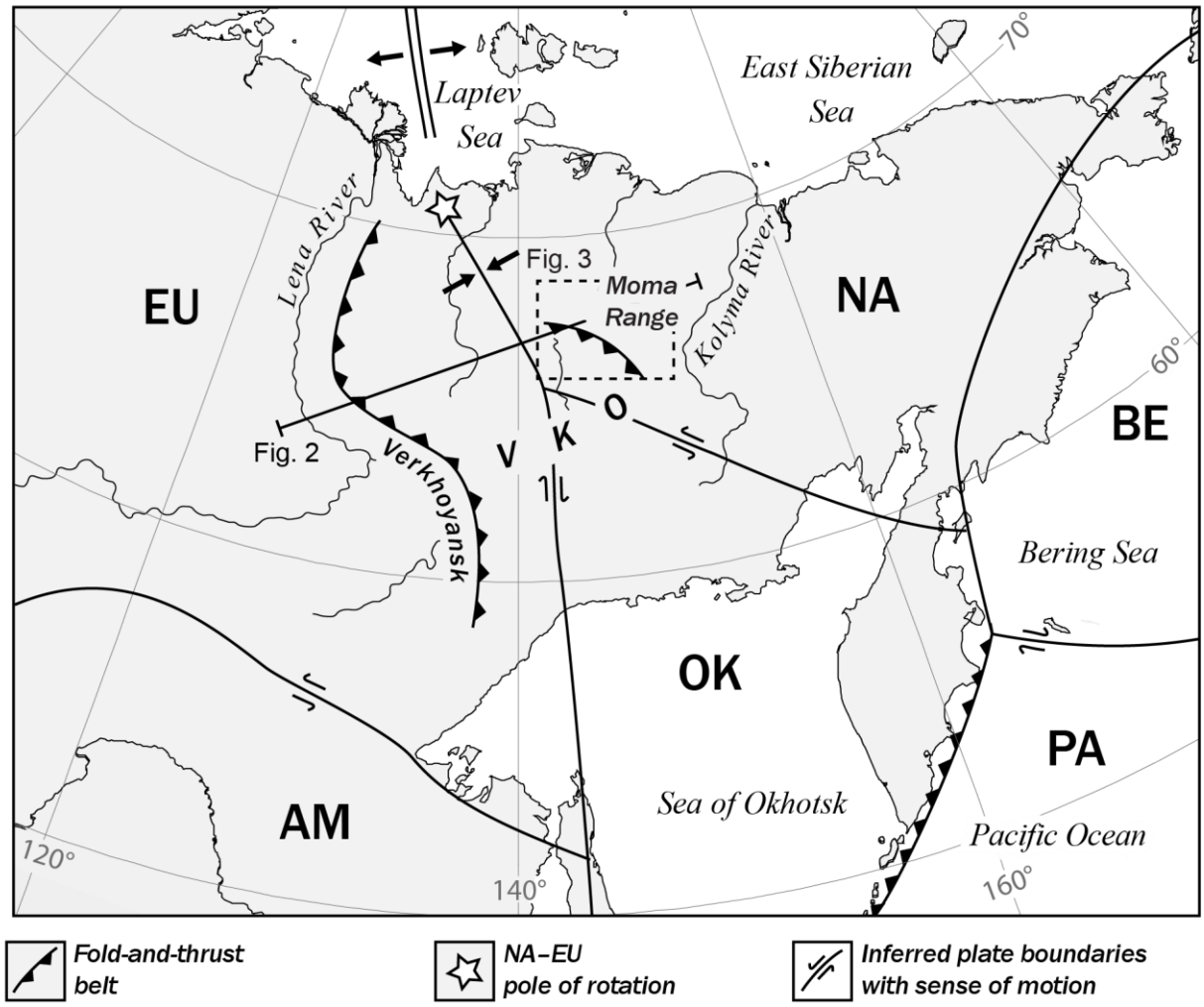

Figure 1. Generalized tectonic and geographic index map of the Verkhoyansk—Kolyma orogen (VKO) showing major tectonic plates (North America (NA), Eurasia (EU), Okhotsk (OK), Pacific (PA), Amur (AM) and Bering (BE)). Star denotes Cook et al. (1986) NA–EU pole of rotation.

Research on the present-day geodynamics in northeast Russia has concluded that Eurasia and North America are currently converging (e.g., Cook et al., 1986; Parfenov et al., 1988; Fujita et al., 2009), but few (Gaiduk et al., 1990; Imaev, 1991) have suggested that either of the fold-and-thrust belts are currently active. This is likely because both fold-and-thrust belts are at significant distance (> 150 km) from where the plate boundaries have been drawn (Fig. 1), and up until recently, the fold-and-thrust belts for the most part have been characterized only by microseismicity. However, there are a select number of moderate and larger-magnitude (> 5 Mw) events located in the western Moma Range and in the Nel'kan-Kyllakh thrust system of the southern Verkhoyansk (Fujita et al., 2009). The complex tectonic history of the VKO traces back to the mid-Mesozoic (e.g., Parfenov, 1991), and includes the collision of several crustal blocks whose boundaries remain as zones of weakness, partitioning modern strain across a broad area.

The objective of this research is to combined geomorphology with remote sensing to examine stream profiles and channel morphologies in the Moma Range fold-and-thrust belt to help delineate the surface expressions of active deformation. Additionally, I explore the ability and limitations of obtaining meaningful information on the tectonics of an inaccessible region, where uplift rates and active structures are largely unknown, without going in the field.

2. TECTONIC EVOLUTION AND MODERN GEODYNAMICS

2.1 Mesozoic geology

The VKO has developed since ~160 Ma in response to the closure of the Oimyakon Ocean and subsequent collision of the Kolyma-Omolon superterrane with the Siberian craton (e.g., Fujita and Newberry, 1982; Zonenshain et al., 1990; Parfenov, 1991; Oxman et al., 1995; Prokopiev, 2000; Layer et al., 2001). Layer et al. (2001) constrained the tectonic evolution by 40Ar/39Ar geochronology and trace element geochemistry obtained from plutonic belts and individual intrusions sampled within the VKO's interior. It begins with the subduction of oceanic crust beneath the Kolyma-Omolon superterrane in the Middle Jurassic (~160-140 Ma), and the emplacement of subduction related granitoids (Layer et al., 2001) and the devlopment of the Uyandina–Yasachnaya volcanic arc along with its backarc basin, the Ilin'-Tas (Fig. 2) (Parfenov, 1991).

By the Early Cretaceous, the Kolyma-Omolon superterrane collided with the Siberian craton, emplacing the 140-138 Ma collisional granites (Layer et al., 2001). The overlying sedimentary cover detached from the basement in the form of large, outward-vergent fold-and-thrust belts in both east and west directions. In the west, late Paleozoic and early Mesozoic passive margin strata, back-thrust onto the Siberian Craton resulting in the formation of the Verkhoyanask fold-and-thrust belt and Priverkhoyanask foredeep (Parfenov, 1991). The westward propagation of thrusting in the Verkhoyansk Mountains, presumably ended in the Late Cretaceous (Prokopiev, 2000). The eastward propagation lead to the inversion of the Ilin'-Tas basin and the uplift and development of the Moma Range fold-and-thrust belt (Fig. 2) (Gaiduk et al., 1990; Gaiduk et al., 1993; Gaiduk and Prokopiev, 1999). The timing and evolution of this

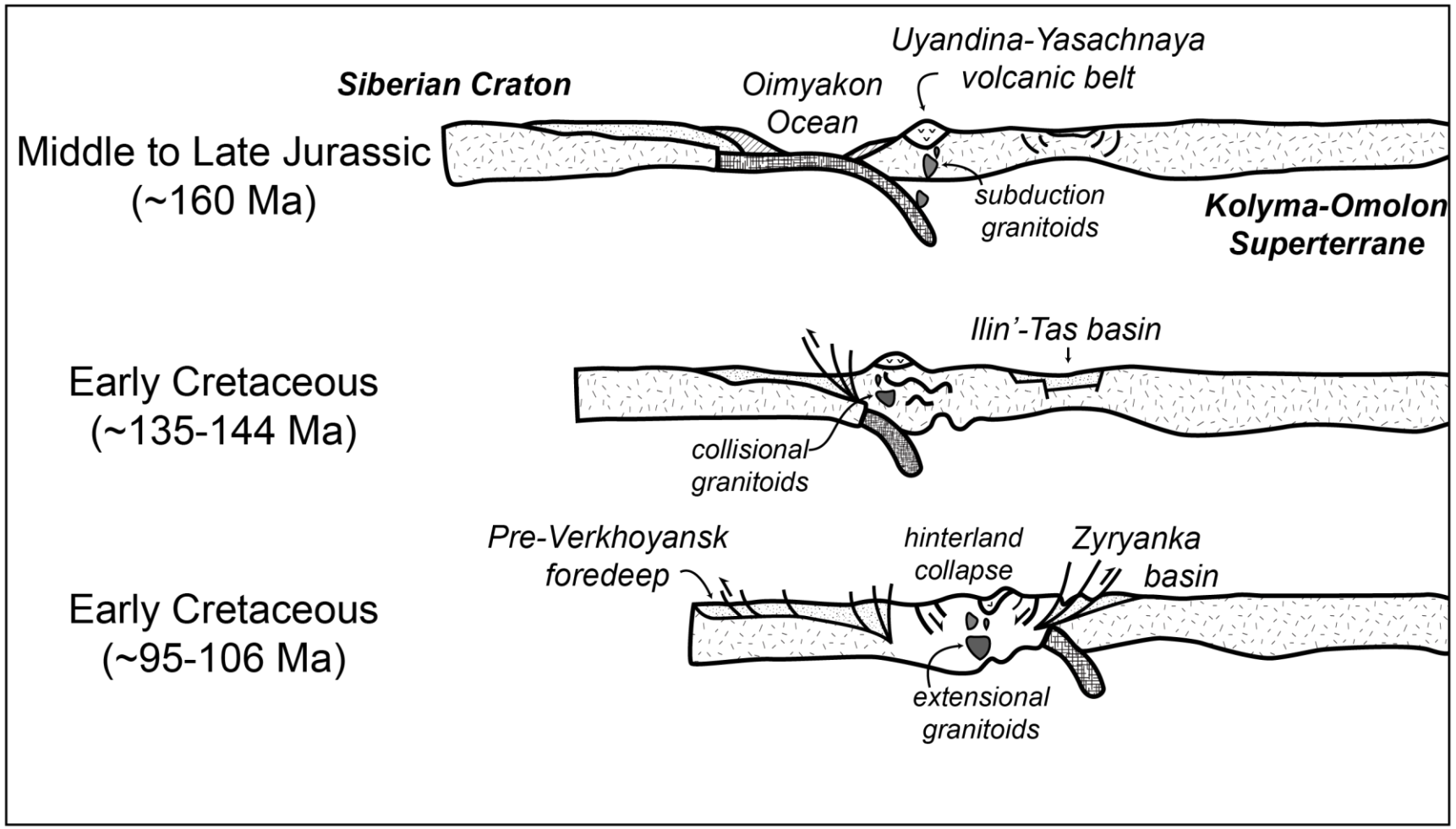

Figure 2. Tectonic evolution of the Verkhoyansk—Kolyma orogen (VKO). Modified form Parfenov (1991) and Layer et al. (2001).

event is unclear. Most authors recognize a Late Cretaceous folding event (e.g., Parfenov, 1991, Prokopiev, 2000; Peach, 2009).

Subsequent to, and possibly concurrent with, the Late Cretaceous outward propagation of the fold-and-thrust development, Layer et al. (2001) suggest a late-stage, east-west extensional event that emplaced several granites and a series of north-south oriented dikes. They speculate that the extension is related to the far-field back-arc effect of Okhotsk–Chukotka volcanic belt or the more intermediate-field effect of the north-south closure of the South Anyui suture. A third explanation for the Late Cretaceous extension is a hinterland collapse model, where the sufficiently thickened crust of the VKO collapses under its own weight, laterally spreading out and adding to the outward propagation of fold-and-thrust development (Fig. 2).

2.2 Cenozoic geology

The history of Cenozoic deformation in the VKO is poorly constrained, and several models regarding its tectonic evolution exist. One model argues that collisional tectonics, initiated in the Mesozoic, persisted until Quaternary time (Gaiduk et al., 1993; Gaiduk and Prokopiev 1999; Fridovsky and Prokopiev, 2000; Paech, 2009). The evidence for prolonged Cenozoic compression is minimal, but thrust structures in the northern foothills of the Moma Range displace Late Cretaceous strata onto Oligocene-Miocene strata, lending to a late Cenozoic shortening event (e.g., Gaiduk et al., 1990; Gaiduk and Prokopiev, 1999).

A second model includes a relatively short-lived period of middle Cenozoic riffing, possibly associated with the protrusion of the Gakkel Ridge into the Asian continent (Cook et al., 1986; Parfenov et al., 1988; Fujita et al., 1990; Calais et al., 2003, Teschegg et al., 2011). This is supported by series of large topographical depressions within the eastern VKO (e.g., Moma–Selennyakh, Uyandina, Ust-Nera, Seimchan–Buyunda). These depressions are intermontane and

filled with Neogene to Paleogene strata (Grinenko et al., 1999). The largest of these is Moma–Selennyakh depression (~16,000 km^2, Fig. 3), and it is situated geographically between the Chersky and Moma ranges.

In addition to topographical depressions, seafloor magnetic lineations along the Mid-Atlantic and Gakkel ridges reveal that the North America and Eurasia pole of rotation was situated in the southern VKO during the middle Cenozoic (Savostin et al., 1984; Gaina et al., 2002; Merkouriev and DeMets, 2008). It is likely that this southern sift of the pole of rotation triggered the middle Cenozoic rifting event associated with the topographical depressions and rift-related volcanism.

2.3 Geodynamics

Much of the attention by western scientists has focused on the modern geodynamics of the VKO, in particular, deciphering the present-day tectonic boundary between the North American and Eurasian plates in the region. Nearly 90% of the boundary between North America and Eurasia is well defined; it begins in the North Atlantic Ocean along the Mid-Atlantic Ridge. It traces north into the Gakkel Ridge, the ultra-slow spreading center that bisects the Arctic Ocean (e.g., Snow and Edmond, 2007). From there, the plate boundary penetrates into the VKO, passing near or through its pole of rotation (Cook et al., 1986; Kogan et al., 2000; Calais et al., 2003), where extension in the Arctic transitions to a seismically active, diffuse zone of compression, known as the Chersky Seismic Belt (Parfenov et al., 1988; Fujita et al., 2009). The Chersky Seismic Belt encompasses much of the VKO, but likely extends eastward to northern Kamchatka and southward to Sakhalin Island (Fujita et al., 2009).

Contemporary thought surrounding the tectonic configuration involves three plates: North America, Eurasia, and Okhotsk (e.g., Cook et al., 1986). The major boundaries between

these plates are presumed to occur along a network of large strike-slip faults that occupy the internal regions of the VKO (Kozmin, 1984; Imaev, 1991; Imaev et al., 1994, 1995; Fujita et al., 2009). The most notable of these faults is the Ulakhan, a NW-SE sinistral strike-slip fault that stretches for more than 700 km though the central Chersky Range to the Sea of Okhotsk, which has been proposed to delineate the North American–Okhotsk tectonic boundary (e.g., Cook et al., 1986; Parfenov et al., 1988; Riegel et al., 1993; Seno et al., 1996; Fujita et al., 2009). In the southwestern portion of the VKO a series of north-south striking faults, known as Ketanda fault system (Imaev et al., 1990; Riegel et al., 1993; Fujita et al., 2009), possibly delineates the Eurasia–Okhotsk boundary. In the northern VKO no single fault has been proposed to be the plate boundary; however, all the published tectonic maps draw the North American–Eurasian plate boundary through this region (e.g., Bird, 2003; Fujita et al., 2009).

The present-day geodynamics in northeast Russia are unique in that the pole of rotation between NA and EU, calculated using geophysical data, lie within the plate boundary zone (Fig 1., Cook et al. 1986; DeMets et al., 1990; Kogan et al., 2000; Sella et al., 2002; Calais et al., 2003). The consensus among authors is that North America is converging with Eurasia, with Okhotsk wedged in between. A number of models exist to explain how this "nutcracker" style of motion is accommodated in the VKO. Riegel et al. (1993) and Hindle et al. (2009) hypothesized that Okhotsk is undergoing lateral escape to the southeast along the seismogenic strike-slip faults (e.g., Fujita et al., 2009) that dissect the internals of the VKO. This situation is similar to the westward extrusion of Turkey along the North Anatolian fault zone (e.g., Mckenzie, 1972; Barka 1992), where Turkey is wedged between the converging Arabian and Eurasian plates. In both situations, the convergence between the three plates is accommodated by localized transpression along the internal strike-slip faults.

In this research, I propose that the convergence between North America and Eurasia is not exclusively accommodated by transpression along the strike-slip faults of the VKO. Active shortening in the Moma Range fold-and-thrust belt, generally disregarded by past geodynamic research (with the exception of Imaev's limited work) because of its weak seismicity and significant distance from the plate boundary zone, aids in the accommodation of strain within the VKO. The structures of the Moma Range formed during the collision of the Kolyma–Omolon superterrane with the Siberian Craton in the Mesozoic, and have possibly remained active throughout the Cenozoic or were recently reactivated. Active structures can be identified using geomorphic indicators, derived from remote sensing data, and then integrated into a mechanical model based on Coulomb wedge of Davis et al. (1983).

3. STUDY AREA

Soviet structural field expeditions and oil and gas surveys in the mid 1980's provided much of what is currently known about the fold-and-thrust structures in the eastern VKO (e.g., Gaiduk et al., 1989, 1990, 1993; Imaev, 1991). The region is divided into five main structural provinces, each characterized by a distinctive structure, stratigraphy, and physiography. From south to north, I refer to these as the Chersky Range, the Moma-Selennyakh depression, the High Moma Range, the Zyryanka basin, and the Alazeya Uplift (Fig. 3). The three most northern provinces show elements of a foreland basin system, as defined by DeCelles and Giles (1996), that comprises a fold belt (High Moma Range), thrust zone and foredeep (Zyryanka Basin), and forebulge (Alazeya Uplift) (Fig. 4).

3.1 High Moma Range

The High Moma Range has three sub-provinces: Andrei-Tas, Ilin'-Tas, and Arga-Tas mountains (Fig. 3). Together they cover an area nearly 30,000 km^2 and reach elevations greater than 2,000 m. Transverse drainage is a common feature along both the southern and northern flanks of the range, with v-shaped river valleys that cut into and across the structural grain of the mountain belt. In the High Moma Range the geology consists primarily of two formations, the Ilin'-Tas and Bastakh formations. The Ilin'-Tas formation represents the bottom of the Moma-Zyryanka stratigraphic section (Fig. 5), and consists of Middle Jurassic (Callovian) tuffaceous and basaltic volcaniclastic rocks (up to 850 m thick) (Ivanov, 1985). Outcrops of the Ilin'-Tas are rare, and have only been mapped in the Andrei-Tas and Arga-Tas mountains (Surmilova, 1986). The Bastakh Formation (up to 6 km thick) consists of thin, rhythmically interbedded sandstone and mudstone, and is locally tuffaceous. This is the main unit found in the central portions of the High Moma Range (Ilin'-Tas Mountains).

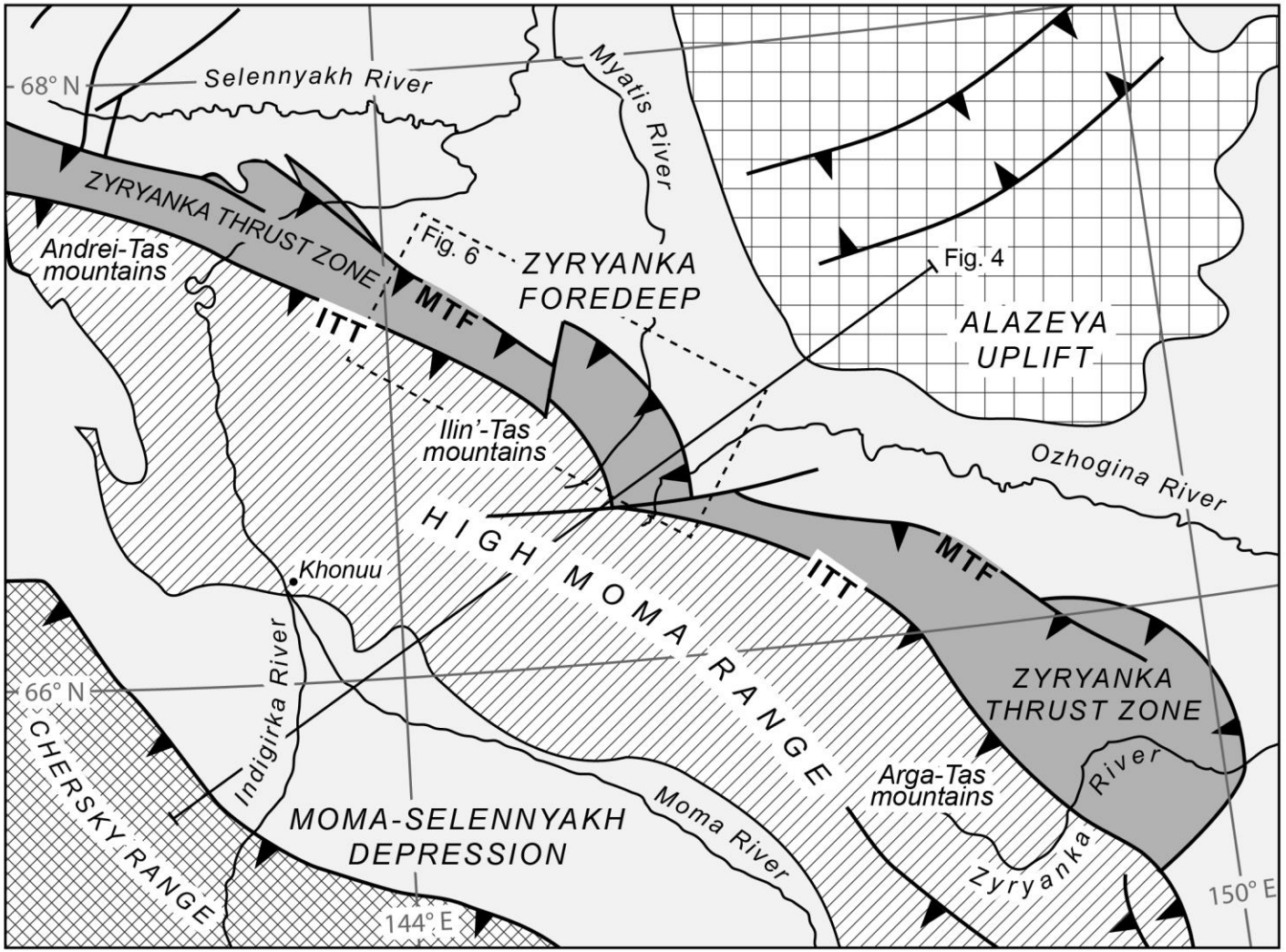

Figure 3. Structural province map (outlined in Figure 1) of the Zyryanka foreland fold-and-thrust belt (modified from Gaiduk et al., 1993). ITT, Ilin'-Tas thrust fault; MTF, Myatic thrust fualt. Thrust faults are represented by teeth on the hanging wall.

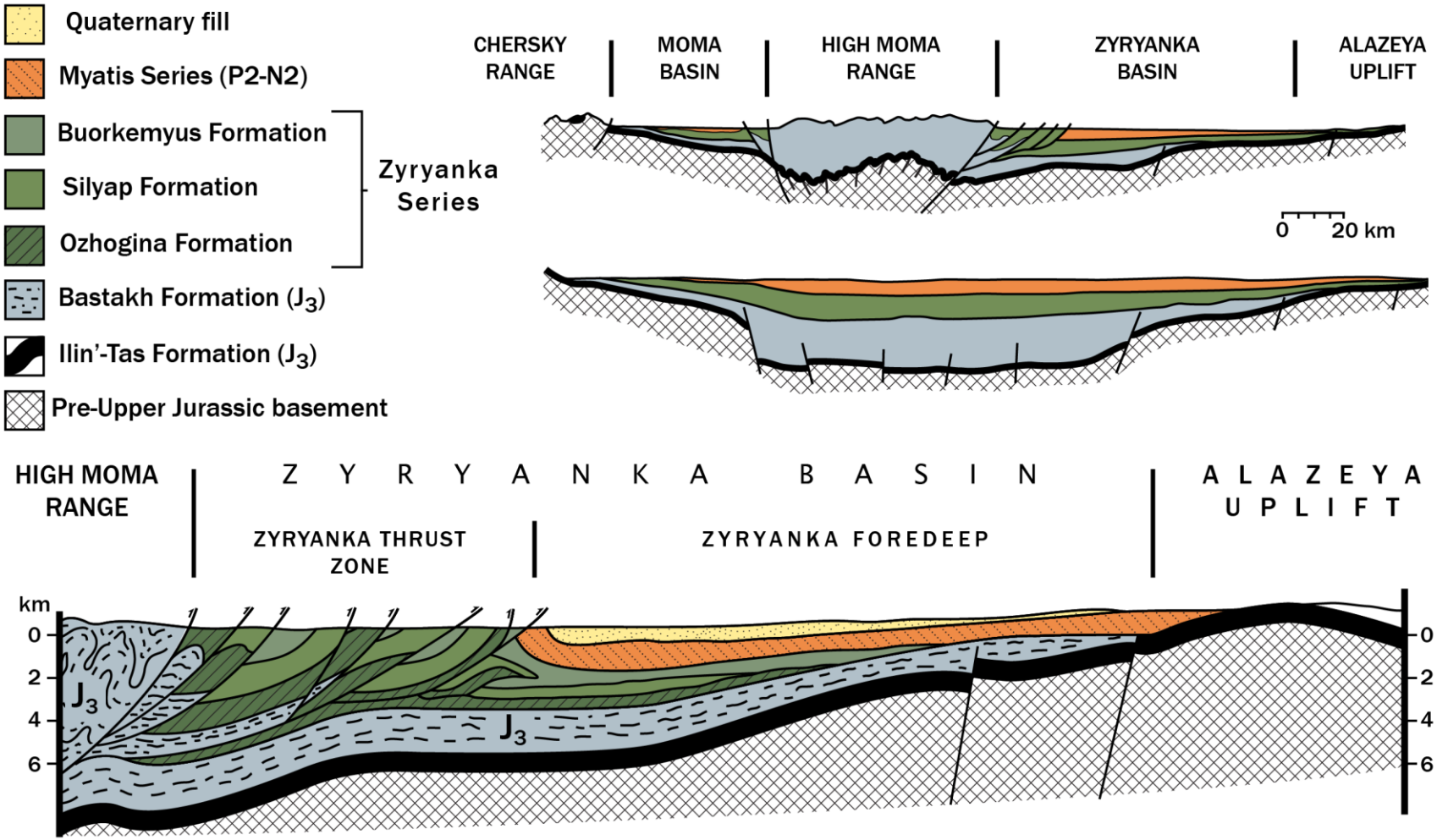

Figure 4. Geologic cross-sections of the Moma Range fold-and-thrust belt (modified from Gaiduk et al., 1990; and Gaiduk and Prokopiev, 1999). Top two sections illustrate a simplified and schematic restoration of the entire region, while the lower section shows the architecture of the foreland fold-and-thrust belt. Lower cross-section begins in the high Moma Range and transverses across the alluvial plain (see Fig. 3). For interpretation of the references to color in this and all other figures, the reader is referred to the electronic version of this thesis

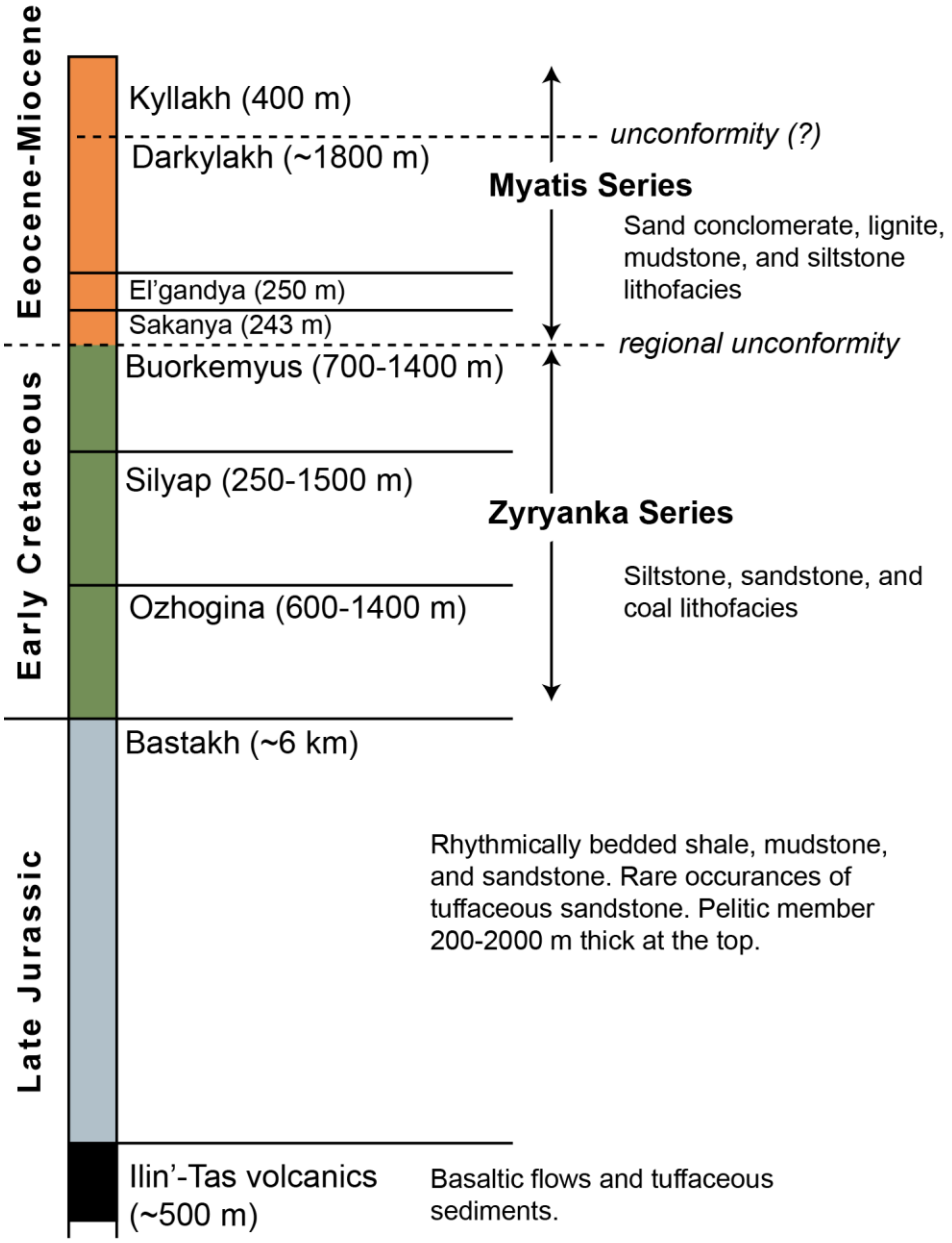

Figure 5. Generalized stratigraphic succession and lithology of Mesozoic and Cenozoic deposits in the Zyryanka Basin (Modified from Ivanov, 1985).

Cross sections published in Gaiduk et al. (1993) and Gaiduk and Prokopiev (1999) bound the High Moma Range by two oppositely-directed overthrusts that penetrate the basement. The fault along the northern boundary is the Ilin'-Tas thrust (ITT), which marks the boundary between the High Moma Range and the northern foothills of the Zyryanka Basin. The south-directed thrust fault, on the back end of the fold-and-thrust belt, lacks conclusive evidence, as some authors favor this as a normal fault associated with the Moma Rift (e.g., Fujita et al., 1990). In the interior of the High Moma Range, the Bastakh Formation is isoclinally folded with steep northeast verging folds. The folding is potentially driven by the reactivation of basement fabrics, such as inverted grabens (Fig. 4) (Gaiduk et al., 1993). However, little is known about the deep crustal structure of the region, and the cross-sections shown here and published in other works are a speculative representation of the region's structure.

3.2 Zyryanka Basin

The Zyryanka Basin is divided into two segments, a thrust zone and a foredeep. The thrust zone segment, commonly referred to as the foothills zone (e.g., Gaiduk et al., 1993), consist of an imbrication of northeast verging thrust sheets that expose early Cretaceous and Cenozoic strata in the northern foothills of the Moma Range. In some localities, the Jurassic Bastakh Formation is included in the thrust sheets. The majority of exposed geology in the thrust zone is the Early Cretaceous strata of the Zyryanka Series (Fig. 5), where three formations are recognized: Ozhogina, Silyap, and Buorkemyus (Ivanov, 1985). The series is several thousand meters thick and consists of sandstone, siltstone, argillite, and coal. Exposed at the very northern edge of the fold-and-thrust belt is the Eocene-Pliocene Myatis Series, where three formations are recognized: El'gandya, Darkylakh, and Kyllakh (Grinenko et al., 1989). The series is

predominately an arenaceous sequence, consisting of sandstone and sand conglomerate, but is locally interbedded with mudstone and lignite in the Darkylakh Formation.

Prokopiev and Gaiduk (1999) provide a detailed geologic map of the eastern half of the thrust zone (Fig. 6), showing several northwest striking, sub-parallel thrust sheets, and two northeast striking tear faults. The outermost thrust sheets are marked by a series of large escarpments that form a salient around the region of the Myatis River, visible in the satellite imagery (Fig. 7). Here the upper member of the Zyryanka Series, the Buorkemyus Formation, is thrust into contact with the lower member of the Myatis Series, the El'gandya Formation, at the southern side of the frontal escarpment (Fig. 4). I refer to this thrust as the Myatis Thrust Fault (MTF), and it likely represents the frontal thrust of the Moma Range fold-and-thrust belt (Fig. 3).

Exposed along the northern escarpment near the Myatis River are the El'gandya and Darkylakh Formations. Here bedding is nearly vertical at the contact with the MTF, and dip angles gradually decrease to the northeast into the foredeep (Paech, 2009; Imaev, 1991). This forms a leading edge monocline at the structural front (Fig. 4) that formed during thrusting along the MTF.

The lateral extent of the thrust zone is not well studied, particularly along the eastern half of the foothills between the Ozhogina and Zyryanka Rivers. Here the thrust zone is presumably much thicker, extending out some 50 km from the topographic front of the hinterland. To the west, the thrust zone extends across the foothills of Andrei-Tas Mountains to the Selennyakh River. Outcrops examined along Bolchuk and Nikandya rivers, correlate with the observed stratigraphy along the Myatis River in the central portions of the thrust zone (Grinenko et al., 1989). The thrust zone widens along this stretch as well, but like the eastern portions of the thrust zone, the structures are not mapped in any detail.

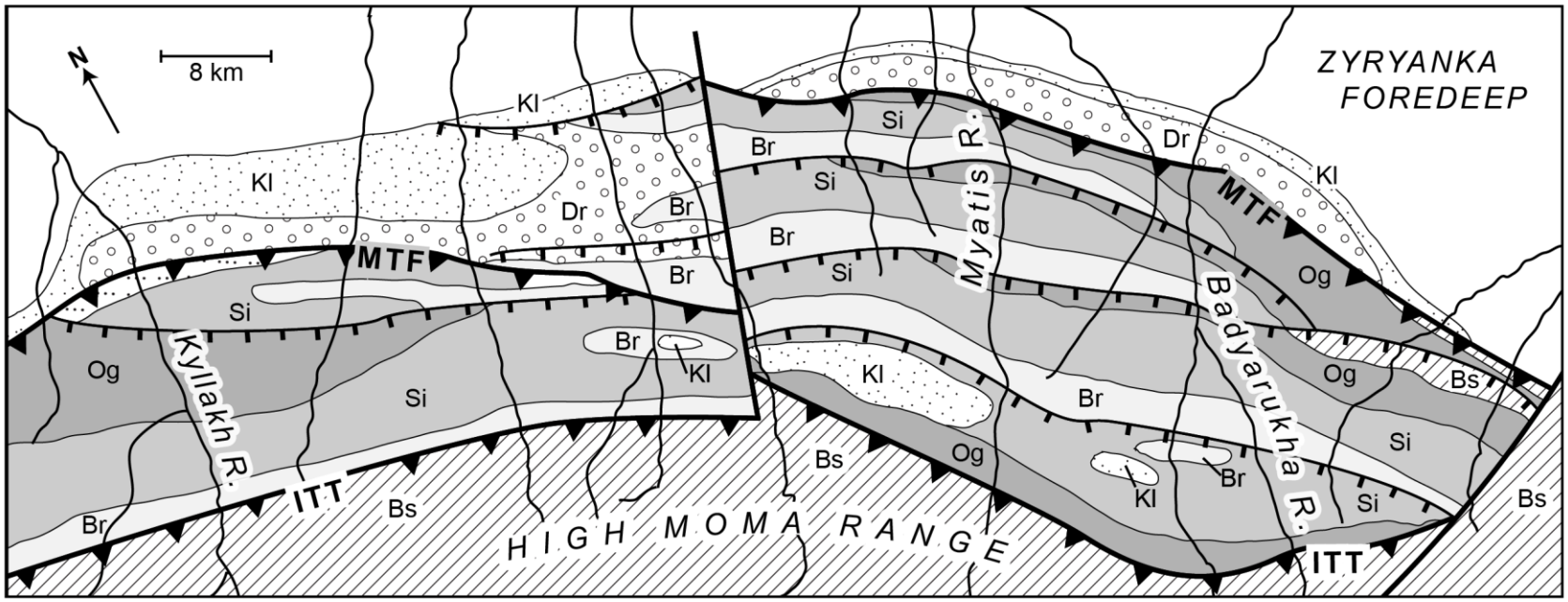

Figure 6. Detailed geologic map (outlined in figure 3) of the Zyryanka thrust zone in the region of the Myatis River. Major thrust faults, Ilin'-Tas (ITT) and Myatis (MTF), are represented by teeth on the hanging wall, while minor thrust are represented with hatch marks on the hanging wall. Geologic units: Bs, Bastakh Group; Og, Ozhogina Formation; Si, Silyap Formation; Br, Buorkemyus Formation; Dr, Darkylakh Formation; Kl, Kyllakh Formation (see figure 5 for stratigraphic succession; modified from Gaiduk and Prokopiev, 1999).

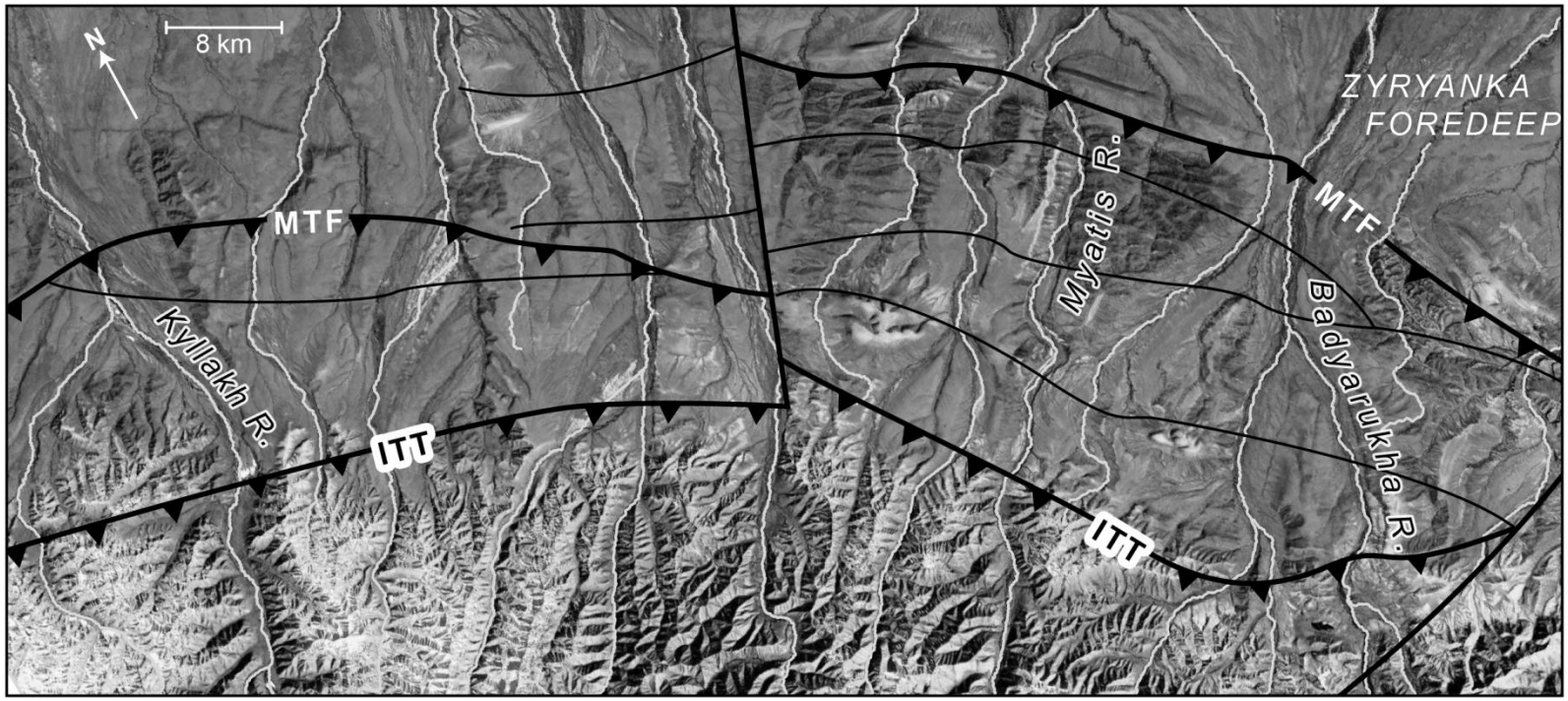

Figure 7. Landsat image of the of the Zyryanka thrust zone in the region of the Myatis River. The MTF is traceable by escarpments in the foothills of the Moma Range, and the ITT marks a distinct transition in the topography. Area is appoximently the same as figure 6.

The Zyryanka foredeep covers an area greater than 60,000 km^2, and the strata exposed in the thrust zone is flat lying and buried beneath a thick Quaternary cover. The depth down to the Upper Jurassic basement is the thickest on the southwest side where it presumably thickens to 4 km (Gaiduk et al., 1989). A series of basement normal faults at the foredeep's northern edge, dip towards the basin's interior (Fig. 4).

At the surface, the foredeep resembles an alluvial plain. In the regions closest to the thrust front, a series of broad fans with radiating drainage patterns extend more the 20 km out from the thrust front. Their slopes do not exceed 0.4°. The Badyarikha River makes the largest of the fans, covering an area of ~650 km^2 with a slope of 0.3° (Fig. 7). The fans appear to decrease in size away from this central region and lose their distinctive fan shape. At the base of the alluvial fans, the surface of the foredeep is characterized by a marshy swampland that covers a large area (>40,000 km^2) and consist of many large lakes.

3.3 Alazeya Uplift

The Alazeya Uplift is a topographically, isolated highland that bounds the northern end of the Zyryanka Basin (Fig. 3). It covers an area greater than 17,000 km^2, and reaches elevations of 600 m. Forebulge uplift has exposed pre-Upper Jurassic basement, presumably of island arc affinity (Parfenov, 1991). Additionally, rocks exposed in the Alazeya Uplift include a series of middle Cretaceous, plutonic, volcanic, and volcaniclastic rocks. Many faults, of various orientations have been mapped in the region, but most of them presumably relate to pre-Cretaceous/Cenozoic deformation. The rivers flow south with dendritic drainage patterns, flowing into the larger rivers (Ozhogina and Badyarikha) in the alluvial plain of the Zyryanka Basin before emptying into the Kolyma and Indigirka rivers.

4. METHODS

Embedded in the Earth's topography is information related to the external and internal forces that shape the Earth's lithosphere. At convergent plate boundaries, shortening of the lithosphere generally produces broad, uplifted mountain belts of steep topography, where surficial processes continually work to level them down. By this observation, it could be hypothesized that mean topographic gradient correlates positively with uplift rates; however, because hillslopes often reach limits in their gradients (Burbank et al., 1996) and uplift in many mountain belts is distributed differentially, the fluvial network is frequently exploited to examine, in more detail, the relationship between topography and tectonic forcing (e.g., Jackson et al., 1996, Kirby and Whipple 2001, Kirby et al., 2003, Lesh and Ridgway 2007, Ponza et al., 2010). Here, I provide an analysis of the rivers that drain the north slope of the Moma Range with a primary focuses on channel morphology, steepness index of individual rivers (k_{sn}), and disturbances in stream profiles (knickpoints). Due to the inaccessibility of the region, digital and analog topography and satellite imagery constitute the major datasets for this tectonic geomorphic analysis.

In northeast Russia, the best resolution of topographic data publically available are the 1:200,000-scale Soviet military topographic maps, which recently have been converted into a 68 m digital elevation model (DEM) that spans all of Russia (www.viewfinderpanoramas.org). Other elevation datasets, such as NASA's Shuttle Radar Topography Mission (SRTM) and the Advanced Spaceborne Thermal Emission and Reflection Radiometer (ASTER), are inadequate for topographic analysis in northeast Russian because of the lack of coverage (north 60° latitude for SRTM) and excessive data holes caused by cloud cover and abrupt changes in topographic relief.

The best available satellite imagery of the Moma Range is the EarthSat NaturalVue 15 m resolution color imagery that nearly covers the entire land area of the Earth. The imagery is derived from images taken by NASA's Landsat 7 satellite, and is constructed by merging a 15 m high-resolution panchromatic band, a 60 m thermal infrared band, and six 30 m multispectral bands to create a single high-resolution color image. The images are orthorectified, mosaicked, and color balanced to create a digital image that is seamless, accurate, and can be used in various mapping software like ArcGIS (available at: http://raster.arcgisonline.com/arcgis/rest/services/MDA_NaturalVue_Imagery/ImageServer).

4.1 Channel morphology

Abrupt changes in channel morphology are often associated with active tectonics, particularly if morphologic changes correspond to areas of increased stream gradient or areas where tectonic structures have been mapped. Numerous stream table experiments have indicated that channel shape is a product of several competing controls, including sediment load, flow velocity, and stream power (e.g., Shumm, 1986). In a particular stream table experiment, a propagating fold was induced across the midsection of an established channel (Ouchi, 1985). It was noticed that in the section immediately downstream from the fold axis, the channel increased its sinuosity, drastically changing its shape (Fig. 8). The increased sinuosity becomes coupled with incision, leaving behind a sequence of terraces (Fig. 8, Ouchi, 1985).

Changes in channel morphology have been identified in tectonically active landscapes from around the globe (e.g., Bullard and Lettis, 1993; Lesh and Ridgeway, 2001; Amos and Burbank, 2007), and they have illustrated a diverse fluvial response to active tectonic forcing. Amos and Burbank (2007) noted that streams undergoing low uplift rates or streams with large drainage areas tend to adjust to differential uplift by narrowing their channel widths, and tend to

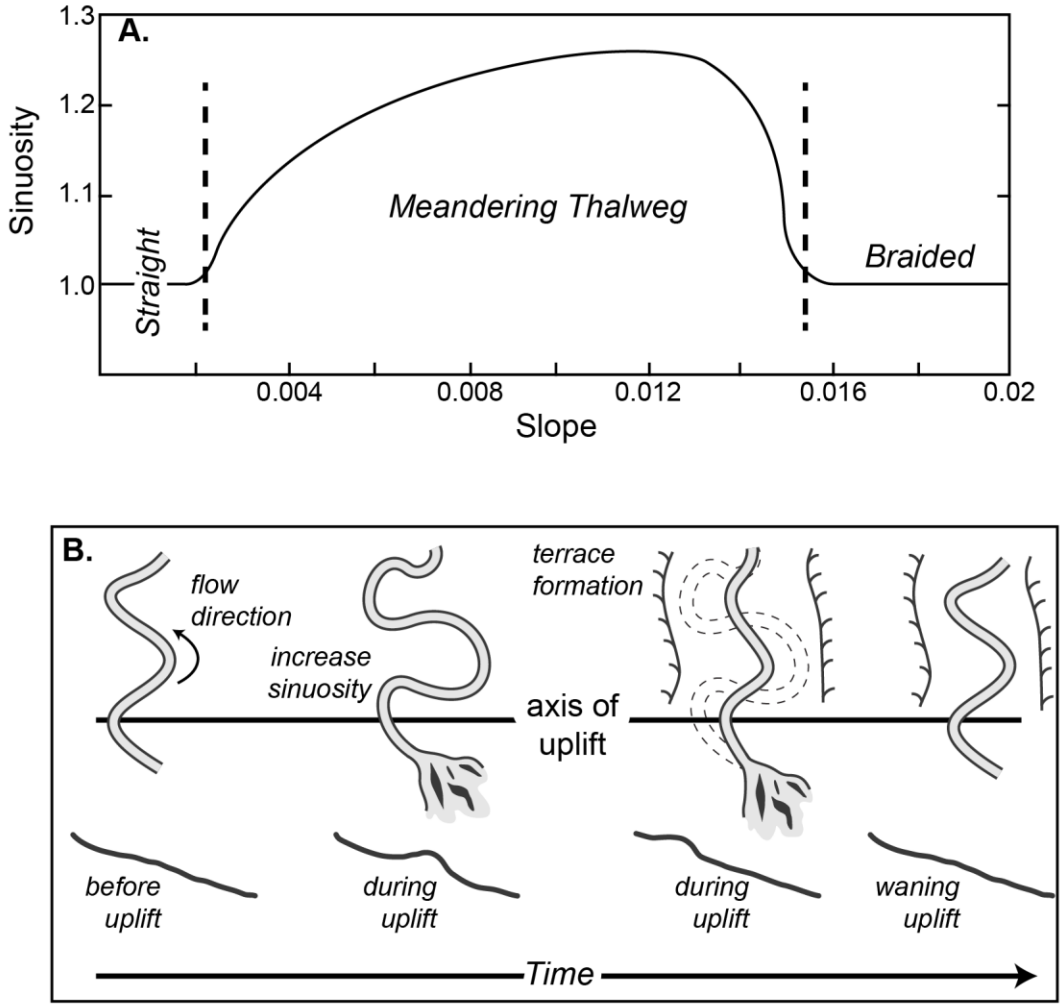

Figure 8. A. Channel sinuosity plotted as function of channel slope (modified after Schumm and Khan, 1972). B. The schematic response of a mixed-load meandering river to the growth of an anticline. The localized uplift causes an increase in channel slope on the downstream segment of the fold limb. This triggers an increase in channel sinuosity and is coupled with incision across the fold limb, while the upstream segment drops its sediment load. As time progresses the locus of incision migrates upstream, smoothing the channel profile and eventually establishing the original channel pattern (modified after Ouchi, 1985).

be more incised. Streams undergoing high rates of differential uplift or streams with small drainage areas adjust by steepening their channel bed.

As is discussed throughout this research, there are numerous competing controls on ways in which fluvial systems adjust their channel morphologies apart from differential uplift or tectonic forcing, including sediment load, stream bed lithology, and climatic factors. Using the EarthSat NaturalVue satellite imagery I have identified several examples of changes in both sinuosity and channel widths of some of the large rivers that drain the northern slope of the Moma Range. I use these in combination with the best geological (Surmilova et al., 1986) and geomorphic (Kolpakov, 1986) maps available to constrain possible external factors outside of tectonic forcing.

4.2 Knickpoints in stream profiles

A knickpoint in a stream's profile is an oversteepened reach or segment that occurs along the course of a smooth profile (Fig. 9). Such a steepened reach could develop in the absence of tectonic forcing simply because of differences in the erodability of the streambed lithology: more resistant rocks will tend to underlie steeper reaches of a stream. Tectonically generated knickpoints can be formed through differential folding or faulting at a localized segment along a stream's profile. Thrust faulting that differentially uplifts an upstream segment with respect to the downstream segment will create a knickpoint in the stream's profile by lowering the base level of erosion for the stream below the fault. Across the steepened knickpoint, stream power (the energy expended on the streambed) will increase due to the increased slope, and erosion of the streambed will be enhanced. The effect of this erosion is to cause the knickpoint to migrate or propagate upstream (Fig. 9; Gardner, 1983).

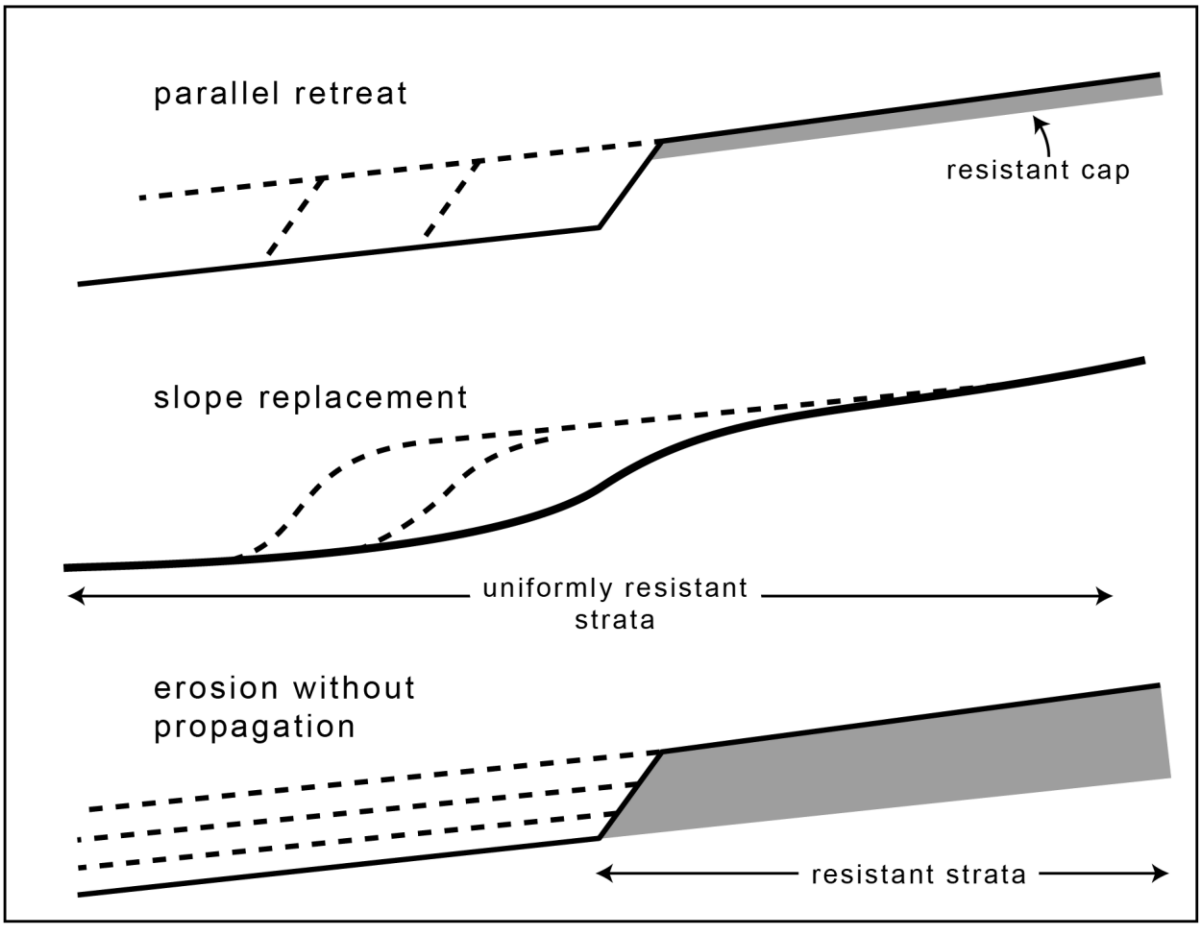

Figure 9. Schematic models of knickpoint migration and morphology for various resistant and nonresistant channel bed material (modified after Gardner, 1983).

Knickpoints are identified within north slope rivers of the Moma Range using longitudinal profiles extracted from the View-Pathfinder 68 m DEM. The method of data extraction is that of Whipple et al. (2007), where it is clearly described. It provides a dual interfaced and user-interactive environment between ArcGIS and Matlab to automate the generation of stream profiles and to retrieve the corresponding slope-area data for individually selected streams. Rivers with very large drainage areas (e.g., the Indigirka and Kolyma rivers) require powerful computers to generate profiles, so some profiles were generated using analog methods (i.e., using the 1:200,000 topographic maps and Google Earth) . The knickpoints are handpicked by observing individual profiles streams and by looking at abrupt changes to trends in the slope–area plots (see following section and Fig. 10).

4.3 Normalized steepness index (k_{sn})

Channel morphologies and knickpoints in stream profiles have relatively short residence times in the geologic record (<10 kyr), and are therefore useful in identifying potential locations of active displacement on faults or growth of folds. However, tectonic processes in northeast Russia, like many other tectonic regions, are slow, and to more accurately understand how the landscape responds to mountain building-scale tectonics, geomorphic processes that operate at more intermediate time scales (>10 kyr) need to be examined. The components pertaining to the shape of a stream profile, the steepness and concavity, are know to reflect the external variables (rock uplift, climate, and streambed lithology) acting on the fluvial system (e.g., Whipple and Tucker, 1999). The profile shapes reflect the long-term landscape processes. Multiple knickpoints may propagate up a given streams profile within the span of 10 kyr. For this reason, stream profiles are widely exploited to gain understanding about the external factors that shape mountain belts (e.g., Kirby and Whipple 2001, Roe et al., 2002; Duvall et al., 2004)

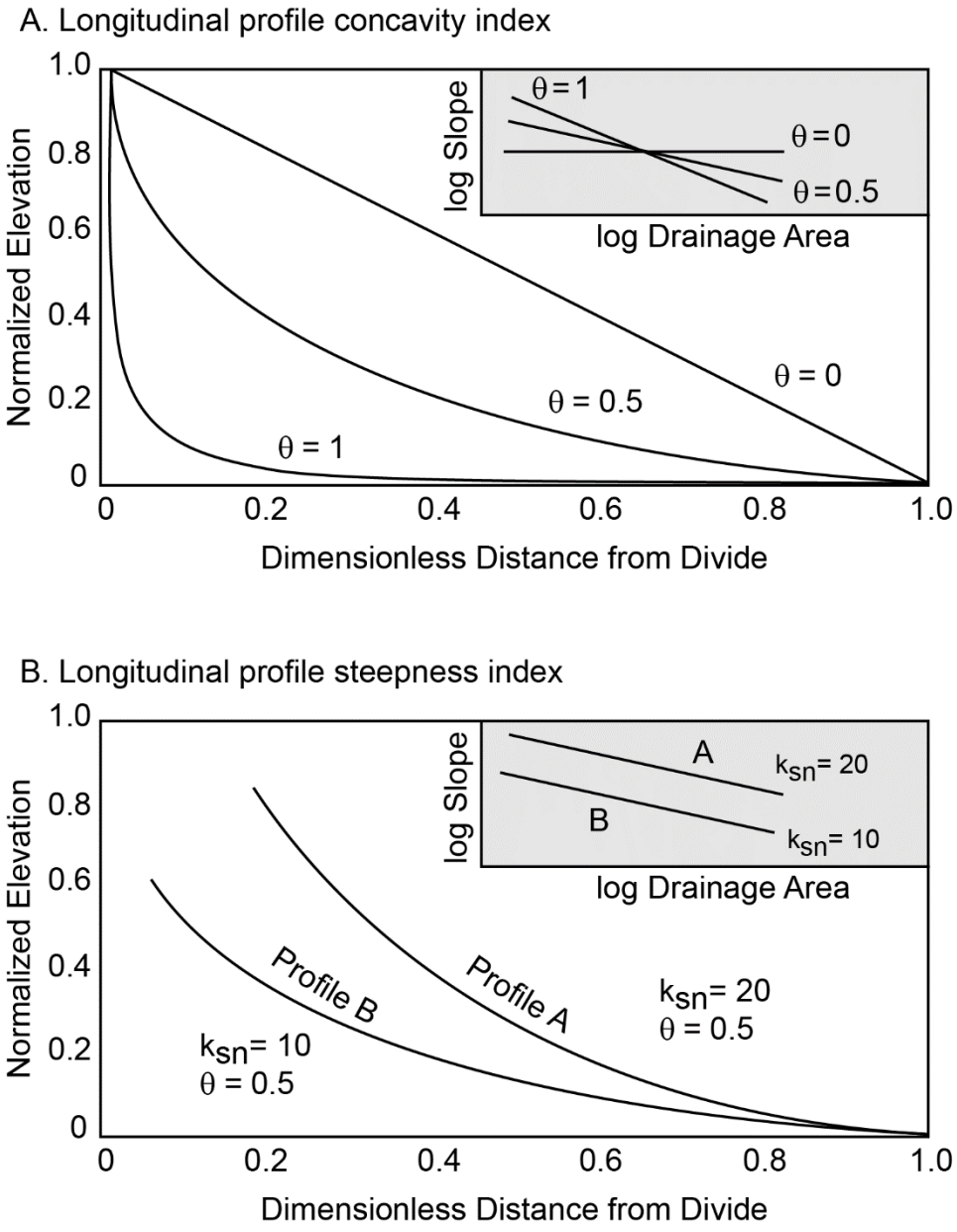

Figure 10. Schematics of equilibrium longitudinal profiles and their derived parameters (modified from Whipple and Tucker, 1999). A. Longitudinal stream profile concavity is set by θ (concavity index). Graph shows how θ values influence profile shape, inset shows how θ values are represented in slope-area space. B. Two profiles with varying steepness indices (k_{sn}). Note that although stream B is twice as steep as stream A, they have the same concavity.

Within the past two decades, drastic improvements have been made to the theoretical and practical methods of stream profile analysis (e.g., Howard et al., 1994; Whipple and Tucker, 1999; Snyder et al., 2000; Whipple, 2001; Wobus et al., 2006). The evolution of a stream's profile is frequently modeled using the detachment-limited concept developed by Howard, (1994), where material eroded from the channel bed is removed entirely from the fluvial system, and bed load transport is not considered. This assumes a fluvial system consisting of bedrock channel beds with little to no alluvium mantle. However, most alpine fluvial systems are characterized by a range channel bed material and sediment transport processes. In the case of the Moma Range, several channel bed properties must be considered when modeling channel steepness, most of which can be dealt with using stream profile concavity (discussed in the proceeding)

Using the detachment-limited concept, it can be assumed that the only controls on a profile's shape are uplift (or base level fall) and erosion.

$$\frac{dz}{dt} = U - E \qquad (1)$$

In equation (1) *dz/dt* represents the change of the stream's elevation, across the entire profile through time, *U* is the uplift rate, and *E* is the erosion rate or vertical incision rate. *E* can be expressed using the vertical incision model proposed by Howard (1994):

$$E = KA^m S^m \qquad (2)$$

where *A* is the drainage area in km^2, *S* the stream's gradient, *K* the erodibility coefficient of the channel bed, and *m* and *n* are constants related to hydraulic geometry and basin hydrology. At steady state (*dz/dt* = 0, i.e., when vertical incision and uplift are in equilibrium), equations (1) and (2) can be combined and solved for *S*.

$$\left(\frac{U}{K}\right)^{\frac{1}{n}} A^{\left(-\frac{m}{n}\right)} = S \quad (3)$$

Under steady state, *U*, *K*, *n*, and *m* are constant, and so additional constants are commonly defined:

$$\left(\frac{U}{K}\right)^{\frac{1}{n}} = k_s \quad (4)$$

and

$$\frac{m}{n} = \theta \quad (5)$$

substituting equations (4) and (5) into (3) to yields,

$$S = k_s A^{-\theta} \quad (6)$$

Equation (6), first proposed by Hack (1957), expresses a stream's slope as a power-law function of the contributing drainage area. The constants k_s and θ represent the steepness and concavity indexes of the profile respectively. By plotting individual slope and drainage area values (black crosses on Fig. 11) for a given interval, k_s and θ can be determined by measuring regressions of distributed slope–area data in logarithmic space (y-intercept for k_s and the slope for θ, see Fig. 10) (Snyder et al., 2000; Wobus et al., 2006). Equation (6) holds conditionally only for critical slopes, generally less than 0.2, which represents the transition from debris-flow dominated to stream-flow processes (Fig. 11) (Sklar and Dietrich, 1998).

In streams where the uplift and vertical incision are uniform across the entirety of the stream's profile, one regression line (one value each for k_s and θ) can fit the accompanying slope–area data below a critical slope (~0.2). Streams perturbed by external variables like

tectonic forcing, climate, or changes in streambed lithology, will inherently be characterized by different values of k_s and θ in different segments. In this study, it is these variations that I exploit to obtain tectonic information from the topography of the Moma Range. Using equation (6) as the regression model, where k_s and θ are free parameters, regressions are fit below the critical slope (0.2) to appropriate segments of the individual stream profiles. Those that contain multiple regressions reflect variations in rock uplift rate, climate, and/or streambed lithology. To compare channel steepness (k_s) from profiles across different catchments, a second regression is performed where θ is fixed to a reference concavity (θ_{ref} = .45), thus producing normalized steepness values (k_{sn}) that can be plotted geographically and compared with the values of neighboring streams and can be used as proxy for uplift rates operating at intermediate time scales (Wobus et al., 2006).

In equation (4) there is a direct power-law relationship between uplift (U) and channel steepness (k_s), assuming the coefficient of erosion (K) is uniform across the entirety of the stream (Whipple and Tucker, 1999; Snyder et al., 2000; Kirby and Whipple, 2001). Profile concavity (θ) is generally thought to be independent of rock uplift when spatially uniform (Tucker and Whipple, 2002; Duvall et al., 2004); however, Kirby and Whipple (2001) used profile concavity to mark transition zones from high to low uplift regimes across a fault-bend fold in the Siwalki Hills of central Nepal.

Using the above technique, I modeled channel profile steepness for channels that drain transversely across the north slope of the Moma Range in an attempt to map out the distribution of uplift across the range. I have created three maps that focus on the Ilin'-Tas, Arga-Tas and the

Andrei-Tas mountains. The raw elevation data are smoothed with a 1 km long window. The slope-area data are sampled at an interval of 40 m (the contour interval the DEM was created from). To automate the process, normalized steepness values (k_{sn}) were calculated using a 20 km long moving window parallel to the entire length of the profile.

As stated earlier, the upper bounding limit of the regression analysis is the critical slope (~0.2), while the lower limit is where streambeds are no longer over bedrock (i.e., alluvial-bedded or transport-limited systems), generally when the slopes are very low and/or when drainage area is large (Fig. 11). Commonly associated with the transition from bedrock to alluvial channels is a negative steeping of the slope-area regressions (increase in channel concavity), and generally a theoretically predicted range of concavity indices (θ = 0.3-0.6) is implemented to enforce the detachment-limited model (Snyder et al., 2000).

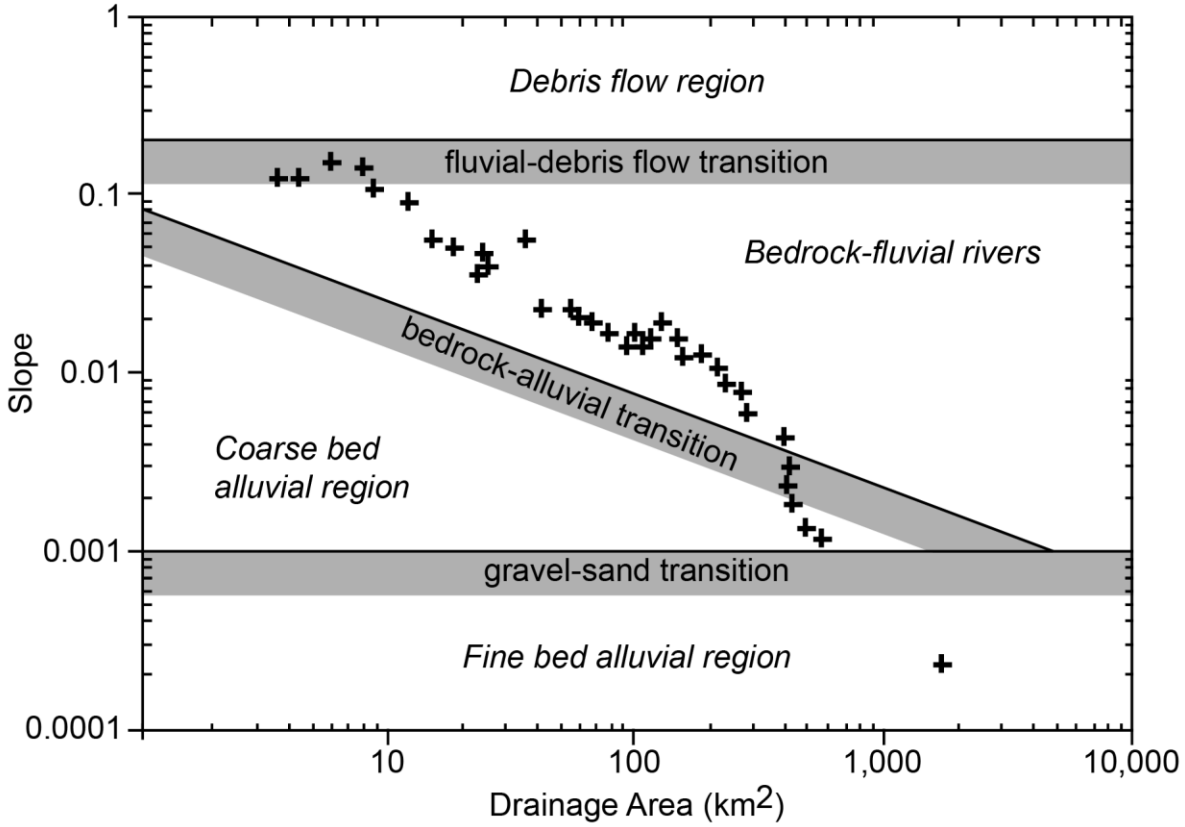

Figure 11. Sample distribution of slope-area data (black crosses) with the classification of stream properties (modified from Sklar and Dietrich, 1998). Note that transitions between classes are gradual and the extent of each class are dependent on the specific grain size and sediment supply rate for any given stream.

5. RESULTS

5.1 Channel morphology

Along the Indigirka River, where it cuts through the western region of the Moma Range (between the Andrei-Tas and Ilin'-Tas mountains; Fig. 3), the largest and most pronounced change in channel morphology occurs. There, the river undergoes an abrupt change in thalweg sinuosity (actual path length/shortest path length), and forms a wide meandering and channelized geometry. The sinuosity changes from ~1.2 in the upstream segment, to ~2.82 in the channelized segment, back to ~1.5 in the downstream segment (Fig. 12). In the channelized segment, the Indigirka River is deeply incised along both of its banks, exposing large outcrops of the Bastakh Group (Fig. 13).

Upstream from the sinuous segment, a series of bedrock capped terraces, over 30 km long, are mapped along the eastern floodplain of the Indigirka (Kolpakov, 1986). Between the eastern terraces and the river, within the floodplain, are a series of noticeable meander scars. On the western bank of this segment, the river is banked up against the Andrei-Tas Mountains, and no terraces are mapped along this side. Near the confluence of the Moma and Indigirka rivers and along the lower reaches of the Ilin-Eselyach River, the major right tributary to the Indigirka, large terraces with broad flat tops sit 200 m above the adjacent floodplains.

On the northeastern slope of the Moma Range, the changes in channel morphology are subtle, and manifest as narrowed channel widths. Channel narrowing can be observed using the satellite imagery along rivers of higher order (e.g., Kyllakh, Myatis, Badyarikha, and Ozhogina; Fig. 14). The best example occurs along the Myatis River, at the border of the High Moma Range and Zyryanka Basin (i.e., at the ITT). Here, the Myatis transitions from what a appears to be a wide,

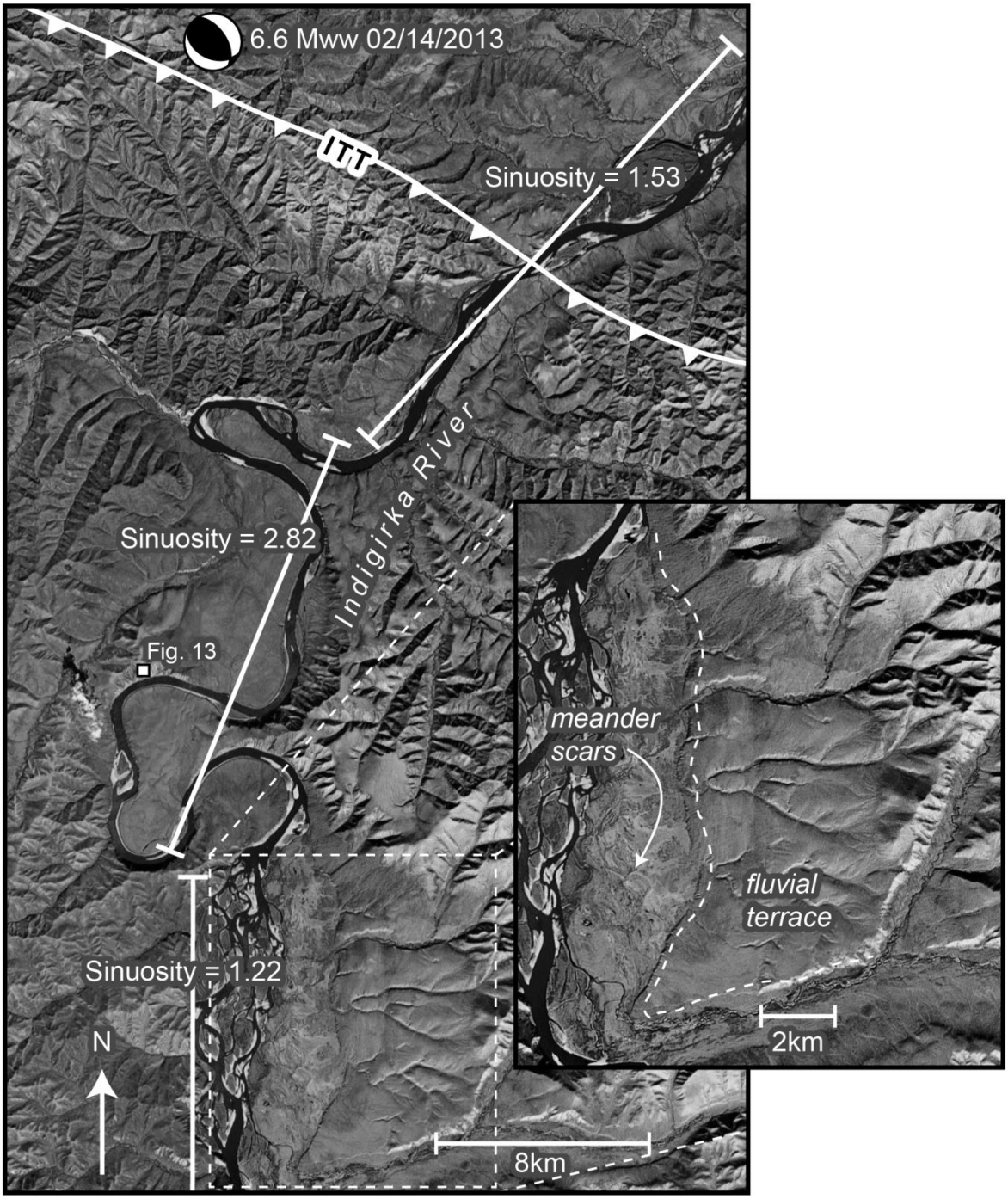

Figure 12. Landsat image showing the abrupt change in thalweg sinuosity of the Indigirka River as it cuts through the the western region of the Moma Range (see figure 3). Inset shows a close up of the eastern terrace sequence and the meander scars along the floodplain. Centroid moment tensor (M_{WW}) from the February 14, 2013 earthquake in the Andrei-Tas Mountains shown in the upper left.

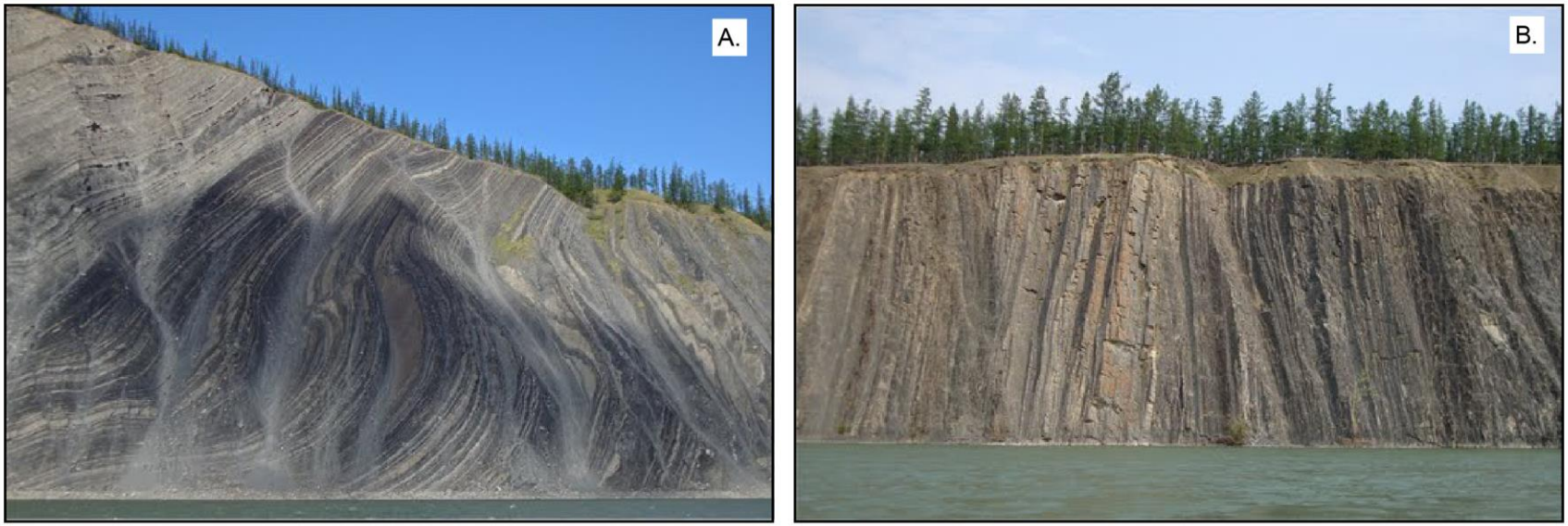

Figure 13. Exposures of the Late Jurassic Bastakh Group along the Indigirka River. A. An exposure along the west bank of the sinuous segment of the Indigirka River (see Fig. 12). B. Upstream from the sinuous segment, showing a bed rock terrace on the east bank of the river. Note steeply dipping and isoclinally folded strata (pictures taken by Yuri Klaver).

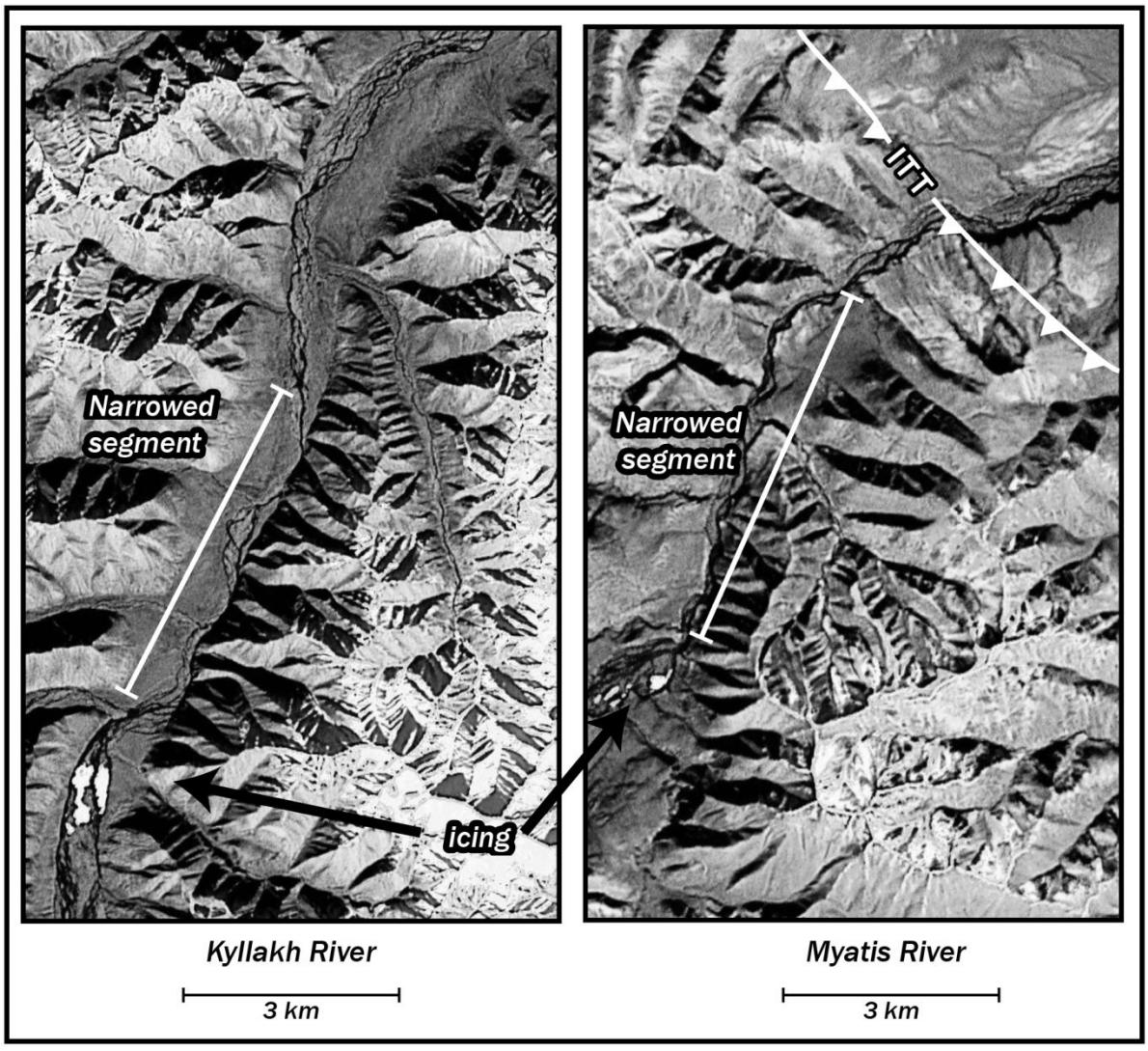

Figure 14. Landsat image of narrowed channel segments along the Kyllakh and Myatis Rivers just south of the Physiographic transition. Note the occurrence of icings upstream of the narrowed channel segments.

almost dammed-up reach into a narrow and incised 5 km long segment, and then back into a more braided morphology as it crosses the thrust zone segment of the Zyryanka Basin (Fig. 14).

5.2 Knickpoints in stream and river profiles

The entire Indigirka watershed (~360,000 km^2) contains a number of large knickpoints located upstream from the Zyryanka foredeep. Figure 15 shows the profile of Indigirka River together with the profiles from two of its large tributaries, the Moma and Selennyakh rivers (constructed using the topographic maps for the elevation and Google Earth for the length measurements), and a map showing the location of the major knickpoints. Along the Indigirka there are three places where there is an apparent break in the slope of the profile (120 m, 400 m, and 600 m elevation, Fig. 15). The knickpoint at the 400 m elevation on the Indigirka is possibly linked with changes in lithology, as this is the location where the river crosses over the batholiths of the Unyandina-Yasachnaya volcanic belt. Along the Selennyakh River, two obvious knickpoints occur in the lower reaches, one at 240 m and another at 350 m elevation.

The Moma River contains the most pronounced knickpoint in the entire Indigirka watershed, and it occurs at an elevation around 500 m. Upstream of this knickpoint, the Moma is a slow, meandering channel, but as it crosses knickpoint it enters a large braided segment (~25 km long and up to 2 km wide), known as the Ulakhan Taryn. Here the channel becomes very shallow, and during the winter months the channel freezes to its bottom and thick sheets of ice can accumulate, leaving portions of the channel covered in ice all year. This phenomena is referred to as a river icing, which are common in Arctic and sub-Arctic watersheds (e.g., Hu and Pollard, 1997), particularly along wide channel segments.

It remains unclear as to what causes these knickpoints. The rivers shown in figure 15 are all large rivers, and they have multiple ways to adjust their channels (e.g., channel narrowing or

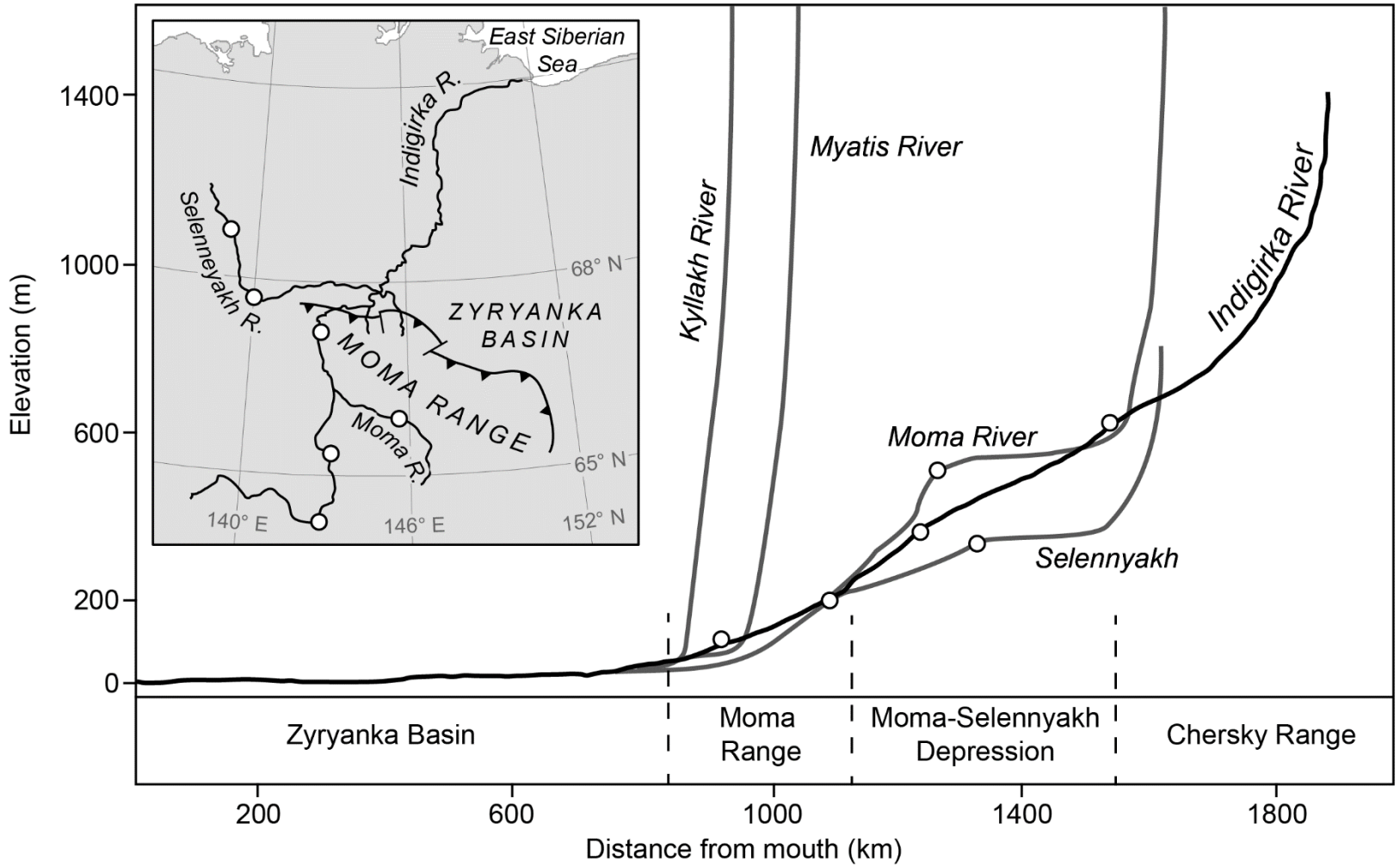

Figure 15. Longitudinal profiles of the Indigirka River and its tributaries. Inset shows the geographical distribution of the large rivers. White dots represent the major knickpoints.

changing sinuosity) to accommodate external forces like tectonic uplift. However, the Moma and Selennyakh rivers make up the major drainages of the Moma-Selennyakh depression, and the knickpoints along these streams are at similar elevations and distances from their confluence with the Indigirka River. This suggest a possible transient link between knickpoints in these tributaries and base-level changes occurring at the lower reaches if the Indigirka River as it crosses the Zyryanka foredeep.

Knickpoints in rivers draining the northern slope of the Moma Range are more subtle than in the large tributaries of the Indigirka. The profile of the Kyllakh appears smooth and unperturbed when plotted along and at the same scale with the larger rivers (Fig. 15), but upon closer examination the profile of the Kyllakh exhibits a large, concave shaped knickpoint just before the Kyllakh enters the Zyryanka Basin. This is one of the largest knickpoints within the north slope streams. The knickpoint is clear in the plotted profile (Fig. 16), and the there is also a significant jump in the trends in the slope–area plots that correlate with the position of the knickpoint. Other rivers that are similar in order or drainage area (e.g. the Myatis River Fig. 17) do not exhibit large knickpoints, and the knickpoints found along these streams appear subdued. Knickpoints are more common in streams with smaller order, but remain difficult to identify (Fig. 18).

Many of the streams in the eastern regions of the Moma Range, in the Arga-Tas Mountains, display knickpoint clusters that are significantly upstream from border between the High Moma Range and the thrust zone of the Zyryanka Basin (e.g., Sibik River, Fig. 19). A northwest-southeast linear trend in the knickpoint locations exists along the upper reaches of a group of streams that originate along Taskan Ridge (north of the Dalekaya River, Fig. 22). The only major knickpoint found in the streams of the western regions, the Andrei-Tas Mountains,

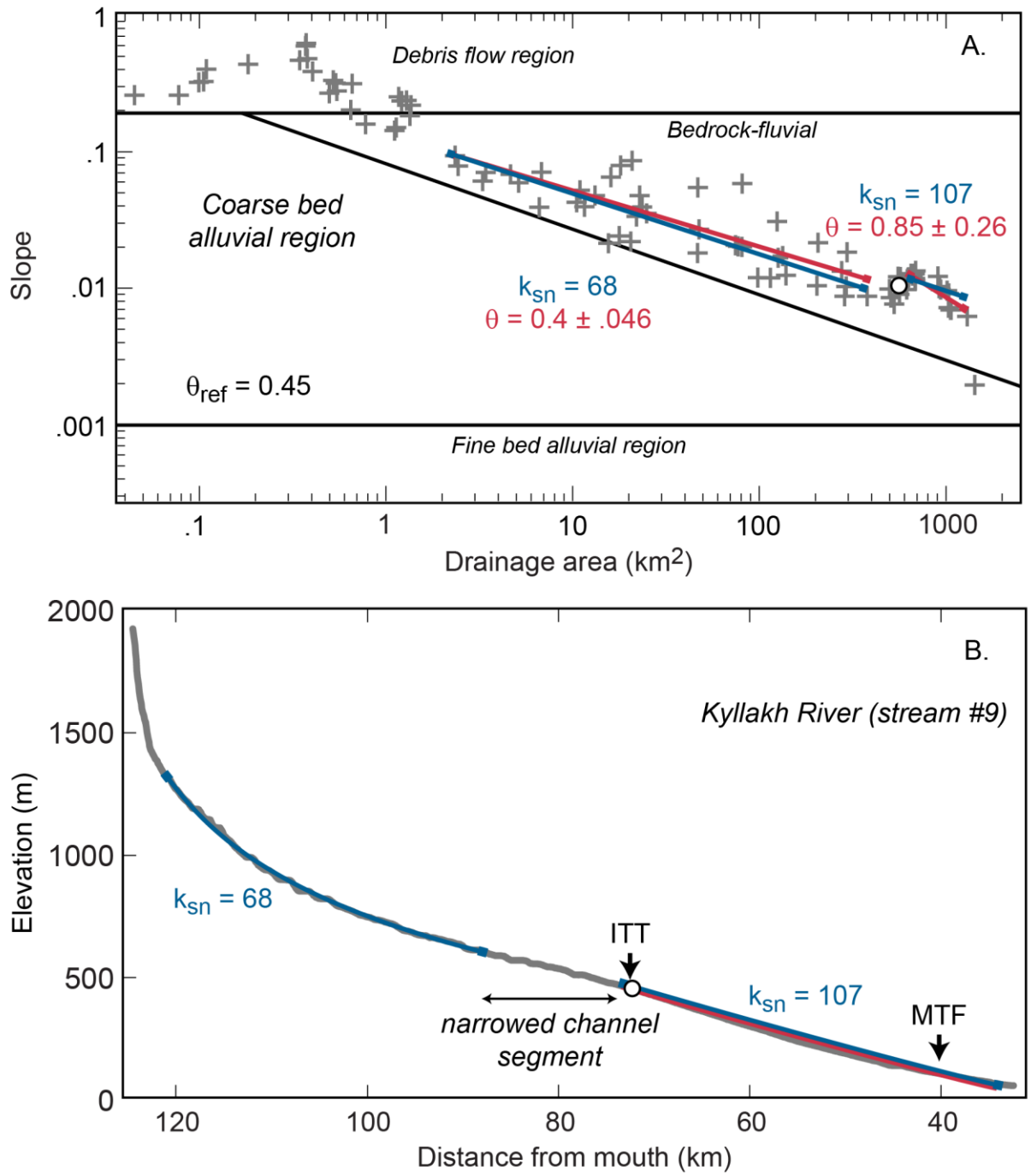

Figure 16. Channel data of the Kyllakh River. A. Slope-area distribution collected from the 60 m DEM. B. Longitudinal profile showing the major thrust faults crossed by the river, the Ilin'-Tas (ITT) and the Myatis (MTF). In both plots blue lines are fits to data with reference concavity (θ_{ref}) of 0.45; red lines are fits to data with concavity as a free parameter

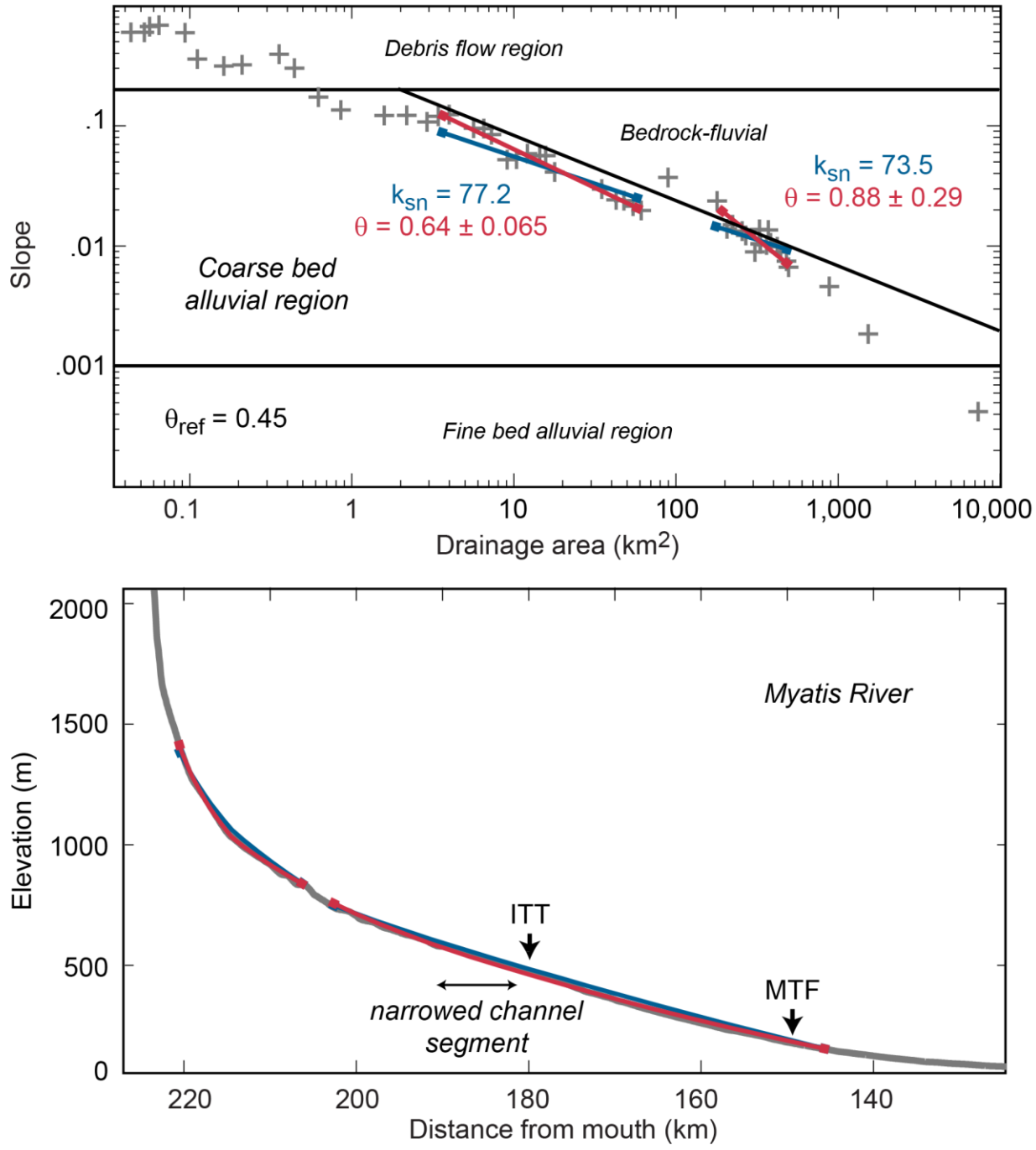

Figure 17. Channel data of the Myatis River. A. Slope-area distribution collected from the 60 m DEM. B. Longitudinal profile showing the major thrust faults crossed by the river, the Ilin'-Tas (ITT) and the Myatis (MTF). In both plots blue lines are fits to data with reference concavity (θ_{ref}) of 0.45; red lines are fits to data with concavity as a free parameter.

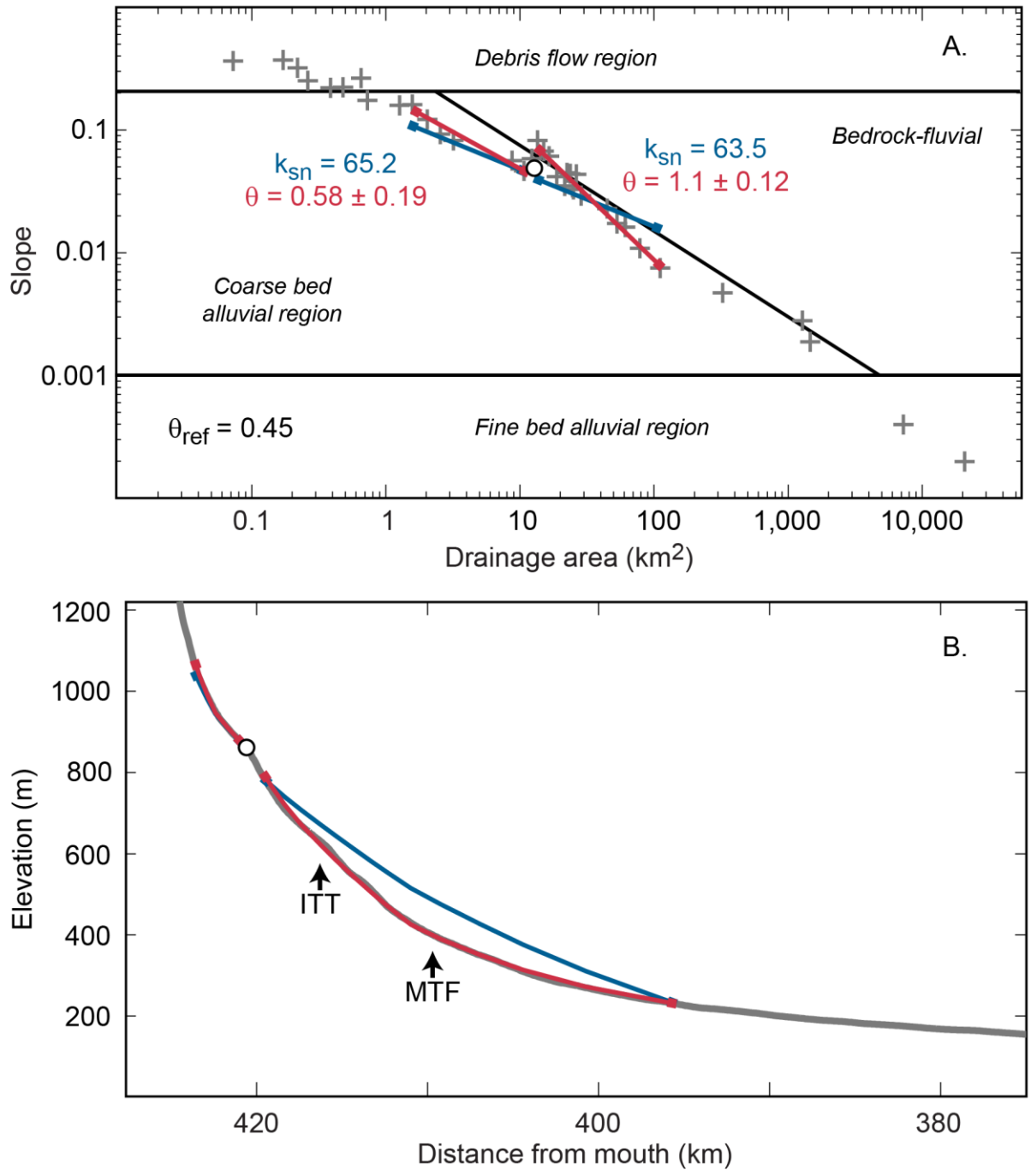

Figure 18. Channel data from a western tributary of the Ozhogina River. A. Slope-area distribution collected from the 60 m DEM. B. Longitudinal profile showing he major thrust faults crossed by the river, the Ilin'-Tas (ITT) and the Myatis (MTF). In both plots blue lines are fits to data with reference concavity (θ_{ref}) of 0.45; red lines are fits to data with concavity as a free parameter. White dot indicates knickpoint in the river.

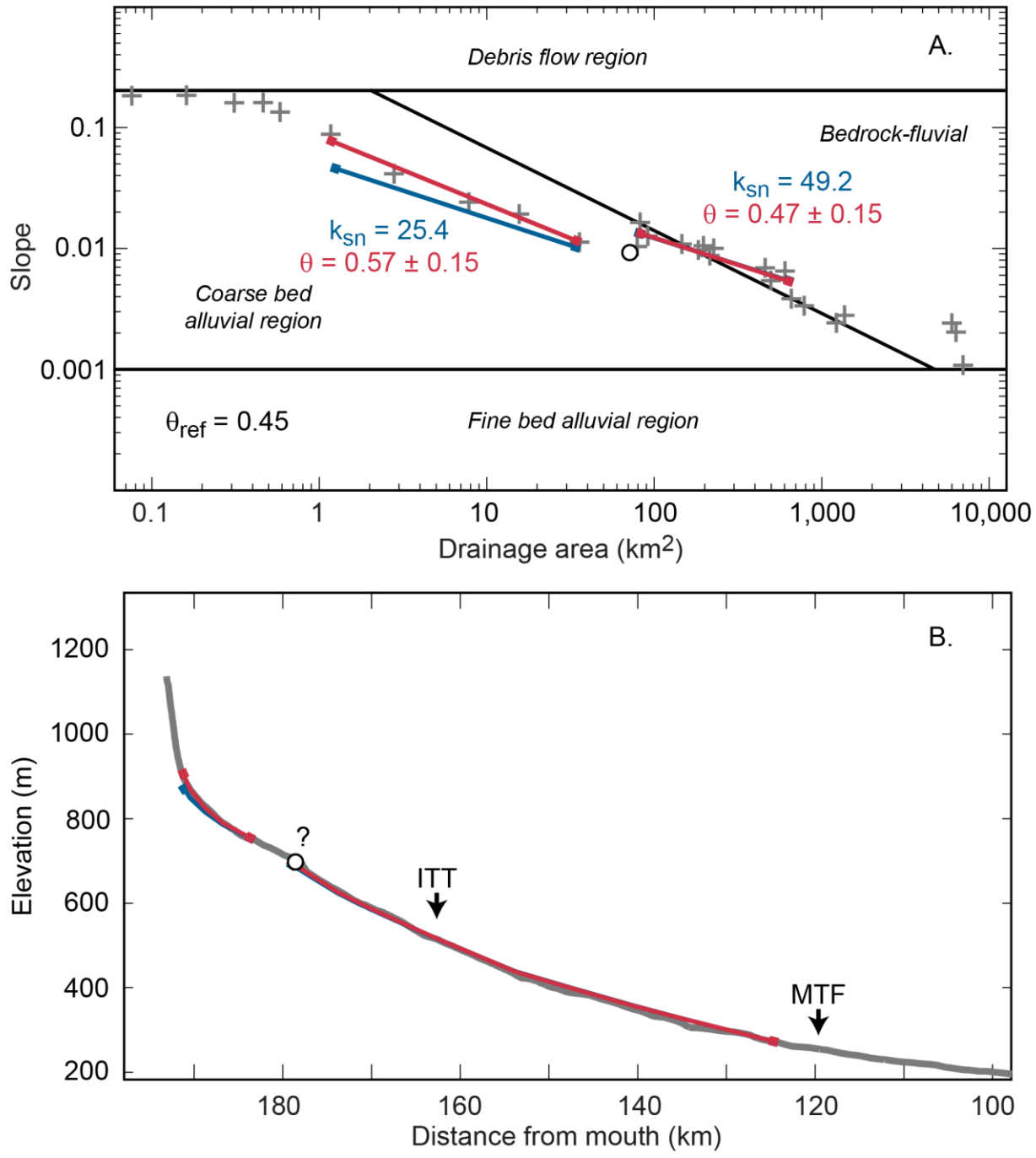

Figure 19. Channel data from a left a tributary of the Zyryanka River (stream #47 Figure 20). A. Slope-area distribution collected from the 60 m DEM. B. Longitudinal profile showing the major thrust faults crossed by the river, the Myatis (MTF). In both plots blue lines are fits to data with reference concavity (θ_{ref}) of 0.45; red lines are fits to data with concavity as a free parameter. White dot indicates knickpoint in the river.

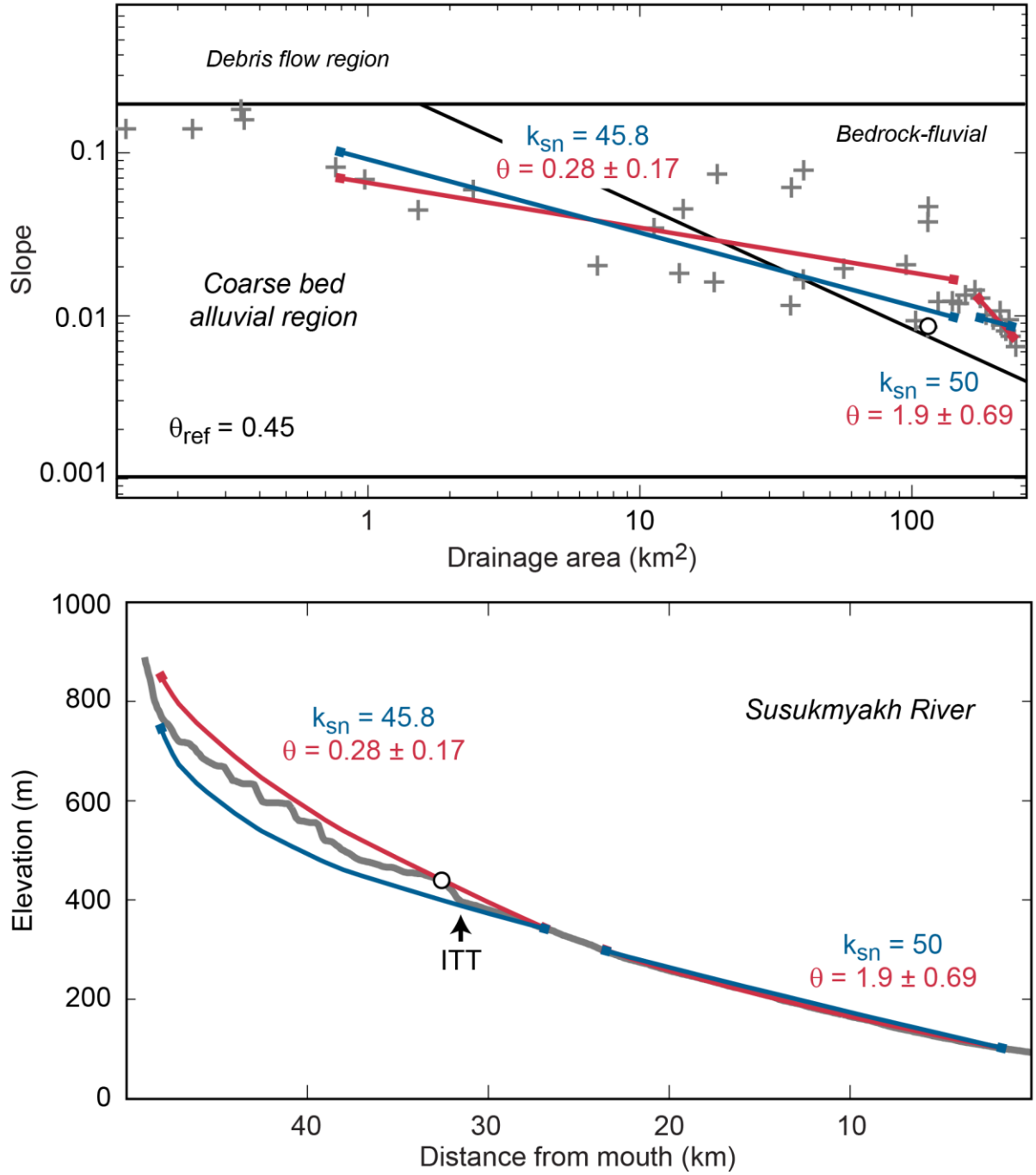

Figure 20. Channel data of the Susukmyakh River. A. Slope-area distribution collected from the 60 m DEM. B. Longitudinal profile showing. In both plots blue lines are fits to data with In both plots blue lines are fits to data with reference concavity (θ_{ref}) of 0.45; red lines are fits to data with concavity as a free parameter. White dot indicates knickpoint in the river. Note the laqrge knickpoint (white dot) just above the Ilin'-Tas thrust (ITT). Other knickpoints shown in profile (stair-step pattern) are artifacts of processing (see text).

occurs along the Susukmyakh River. The knickpoint is at an elevation of ~500 m (Fig. 20), right at the topographic front and the westward continuation of the ITT. Behind this knickpoint is what appears to be a subsequent series of smaller knickpoints; however, these are artifacts of processing from when the elevation data were extracted to construct the profile. Stair-step artifacts like these are common in profiles extracted from DEMs that were built from topographic maps. By going back and referring to the topographic maps, I was able to distinguish between the major real knickpoints, like the one in the Susukmyakh River, and stair-step artifacts.

5.3 Normalized steepness indices (k_{sn})

The magnitudes of the normalized steepness indices for the channel reaches analyzed using the automated approach are plotted as a color-coded maps in figures 21, 22, and 23. These three maps also show the geographical locations of the major knickpoints indentified in this study. The major faults in the thrust zone of Zyryanka Basin, including the ITT and MTF, are shown as a series of black lines that trace along the northern foothills of the Moma Range. The k_{sn} data are classified into five groups, with values >80 and <20 representing the high and low ends of the spectrum respectively. The stream segment with the highest individual k_{sn} value is the upper reach of a right tributary to the Zyryanka River in the Arga-Tas sub-province (126.3). The second highest k_{sn} value (116) occurs along the Kyllakh River, in the segment that includes the major knickpoint (Fig. 16).

In general, channels with larger drainage basins, that have headwaters in the highest regions of the Moma Range have higher k_{sn} values in comparison to the small streams that are

sourced in the foothills. There is also a concentration of high k_{sn} values in the Ilin'-Tas mountains; centered around the region near the Myatis River (Fig. 21).

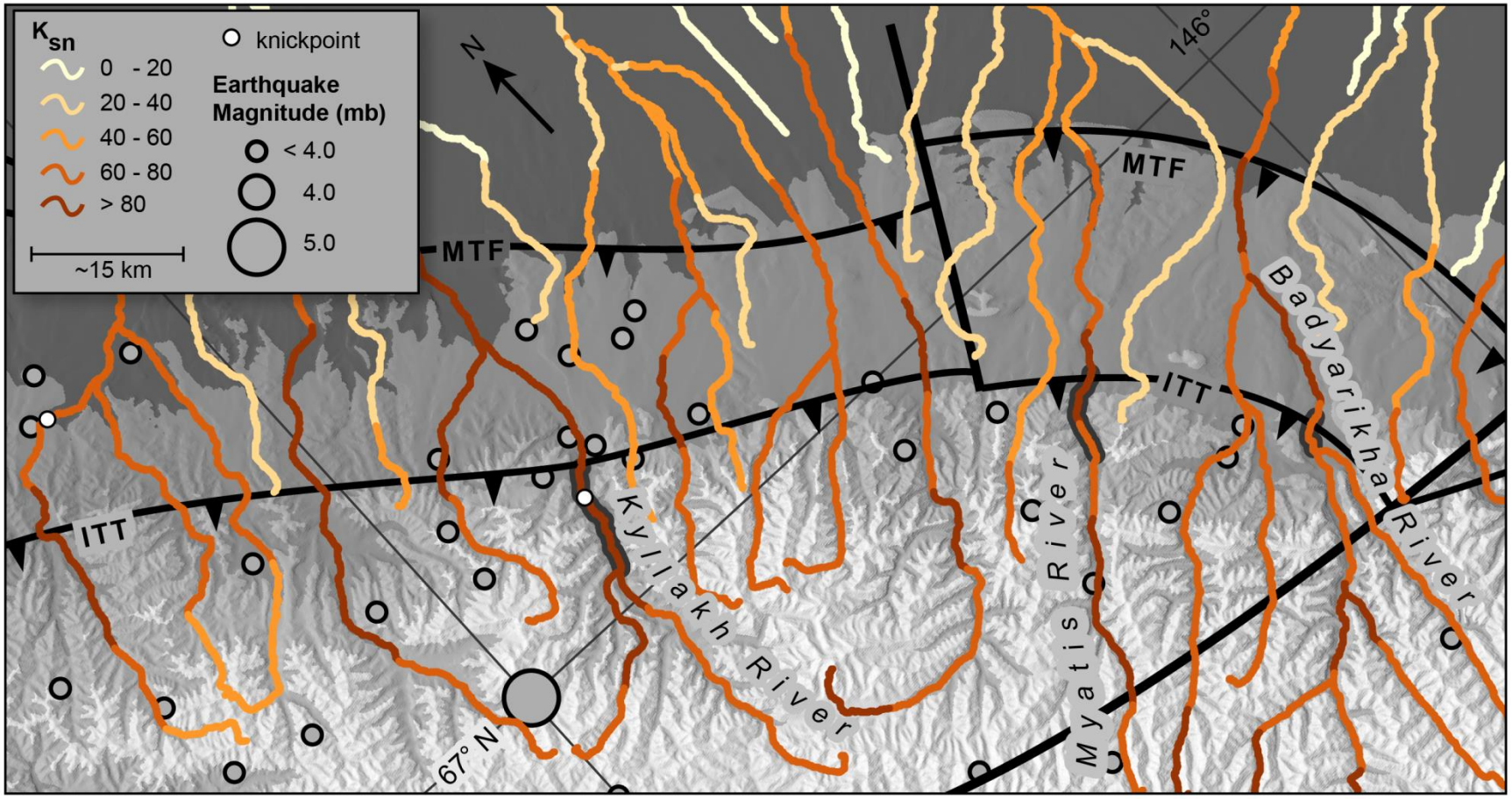

Figure 21. Map of calculated normalized steepness values (k_{sn}) for channels draining the north slope of the Moma Range, in the region of the Ozhogina and Zyryanka Rivers (Arga-Tas sub-province). Values of k_{sn} are color coded to magnitude and plotted over hillshaded topography (provided by www.viewfinderpanoramas.org). Narrowed channel segments are highlighted in dark gray. Major thrust faults, Ilin'-Tas (ITT) and Myatis (MTF) are shown in black with teeth on the hanging wall side. Dashed fault line is an infered structure that is un-mapped.

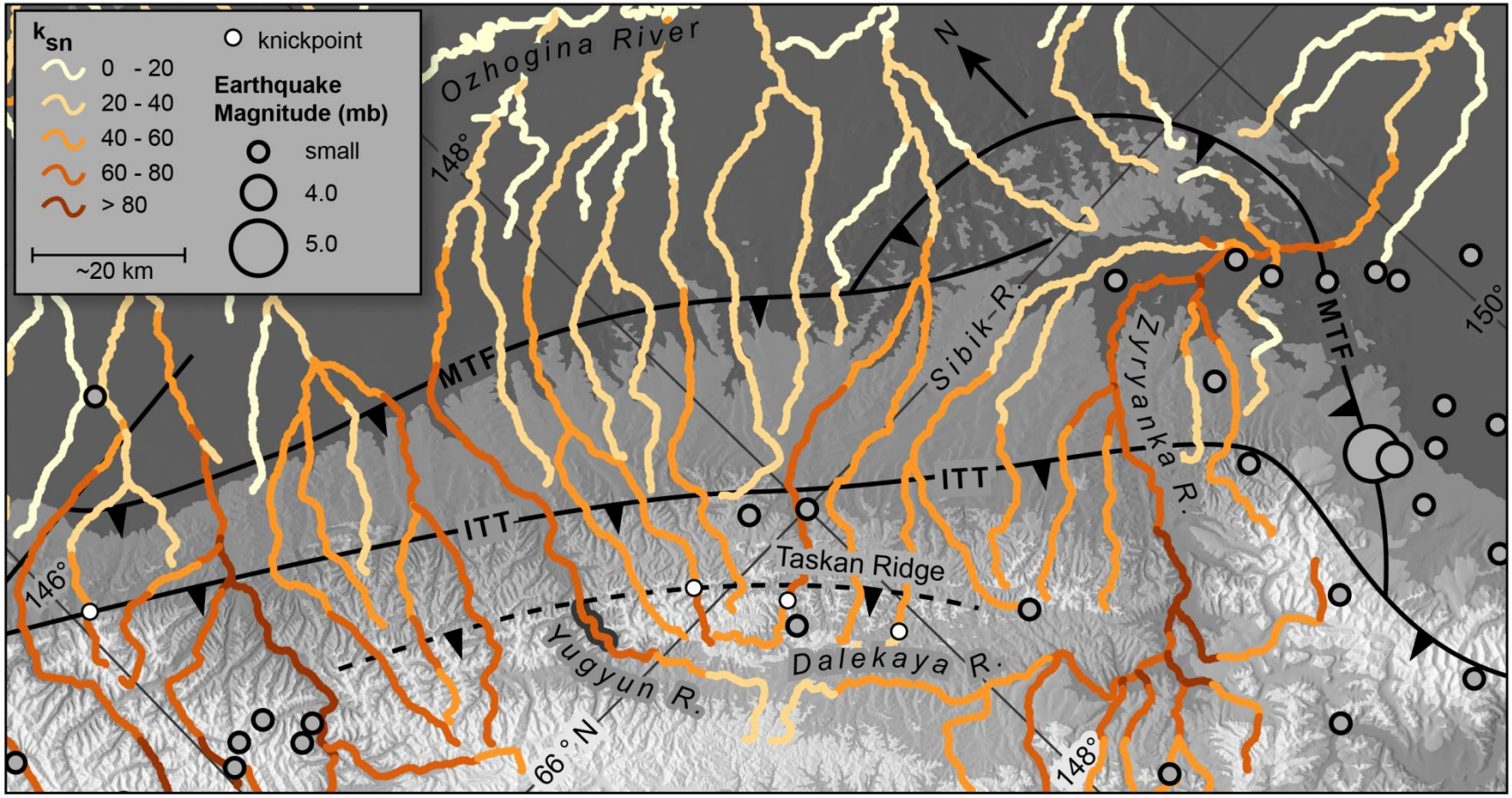

Figure 22. Map of calculated normalized steepness values (k_{sn}) for channels draining the north slope of the Moma Range, in the region of the Ozhogina and Zyryanka Rivers (Arga-Tas sub-province). Narrowed channel segments are highlighted in dark gray. Dashed fault line is an inferred structure along the Taskan Ridge (previously un-mapped)

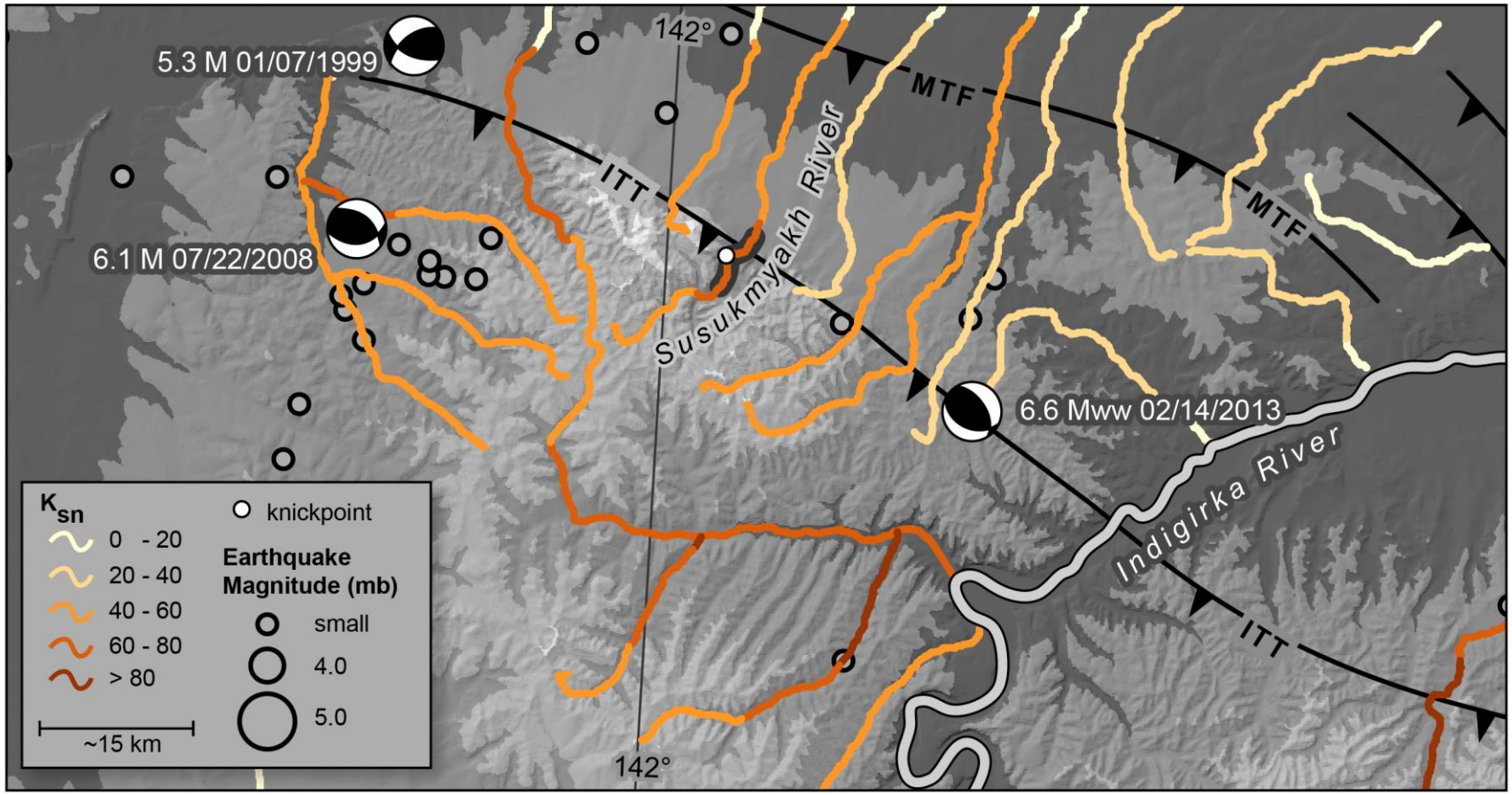

Figure 23. Map of calculated normalized steepness values (k_{sn}) for channels draining the north slope of the Moma Range, in the region of the Andrei-Tas sub-province. Narrowed channel segments are highlighted in dark gray, and the knickpoint in the Susukmyakh River is indicated with a white dot.

6. DISCUSSION

The Moma Range is a Cenozoic fold-and-thrust belt, with vergence to the northeast (e.g., Gaiduk et al., 1990). Many questions remain regarding its architecture and its deformation history, but here I focus on how the fold-and-thrust belt is currently deforming based on the geomorphic indicators. The traditional view of fold-and-thrust belt development consists of a break-forward sequence model, where thrust faults form in-sequence, one after another, initiating in the hinterland and progressing towards the foreland (Davis et al., 1983). If the Moma Range is an actively deforming fold-and-thrust belt, it may be expected that all the current tectonic strain on the Moma Range is accommodated by shear along the frontal thrust, the Myatis thrust fault (MTF); however the data from this study suggest that the portions of the Moma Range are deforming out of sequence, and that thrusting is or recently has been focused along the Ilin'-Tas thrust (ITT).

6.1 Interpretation of geomorphic data

The big jump in thalweg sinuosity of the Indigirka River and its abrupt change in channel morphology as cuts across the interior of the Moma Range, is a clear indication that the Moma Range, in that location, is undergoing uplift. In this case, uplift is triggering an increase in valley slope along Indigirka's channel, and as a consequence the river adjusts its sinuosity to compensate for the change in slope. The change in uplift also causes the channel to incise itself into the landscape, forcing the river into a single channel with steep terraces on both sides. Based on geologic maps (Surmilova et al., 1986), there is no major change in stream bed lithology, and no major tributaries confluence here; leaving a zone of active uplift as the likely candidate for the abrupt change in channel morphology. Bullard and Lettis (1993) drew similar conclusions by observing sinuosity changes in rivers that perpendicularly cross axes of actively growing

anticlines associated with blind-thrust in the Los Angeles basin in southern California. The sinuosity changes measured by Bullard and Lettis (1993) are much smaller in magnitude (~1.06 to 1.24) than the changes measured here (~1.2 to 2.82).

The upstream segment of the Indigirka is characterized by a long sequence of terraces along the eastern floodplain (Fig. 12). I propose that these were formed at an earlier time, when the sinuous portion of the Indigirka was perhaps further upstream (southward). The active zone of uplift may have initiated further back, and the progression of Moma Range deformation and uplift has recently propagated northward. Alternatively, the uplift could be recent and initiating in its current locality with the terraces forming as pre-uplift features; however, timing of such phenomena are currently unconstrained. The meander scars that favor only the right bank of the Indigirka is an indication of an additional westward tilting of the valley floor. Alexander et al. (1994) used similar patterns of meander scars along the Madison River in southwestern Montana to document the direction of tilting of an extensional fault block triggered by the 1959 Hebgen Lake earthquake.

Channel morphology changes for the rivers that transversely drain the north slope of the Moma Range are more difficult to identify. These rivers have much lower stream power therefore making it difficult to cut and erode the landscape, and in turn change their channel morphology. However, several of the higher order streams appear to narrow their channels for short segments (~5 km) near the vicinity of the ITT (Figs. 14 and 21), the bounding fault between the High Moma Range and the Zyryanka thrust zone. These larger rivers are likely gravel bedded in many locations, and when crossing growing folds or zones of differential uplift, alluvial rivers tend to narrow their channels before steepening of the channel occurs (Amos and Burbank, 2007). I suggest that the narrowing of channels is triggered by the active or very recent

differential uplift at the ITT, caused by active thrusting of High Moma Range over the Zyryanka thrust zone.

Knickpoints at these narrowed channel segments are not observed; except for along the narrowed segment of the Kyllakh River, where a large, convex shaped knickpoint is present (Fig. 16). Most of the knickpoints identified in this study occur along low-order channels, and many of them are upstream of the ITT (Figs. 20 and 21), suggesting that vertical displacement along the ITT has at least very recently perturbed the streams that cross it. The knickpoints observed in the large-scale Indigirka profile plot (Fig. 15) may represent the oldest record of base-level fall, caused by the initial subsidence in the Zyryanka foredeep.

In the Arga-Tas Mountains of the Moma Range (Fig. 3), a distinct trend of knickpoints occurs along the northeastern slope of the Taskan Ridge (Fig. 22), and the Yugyun River narrows its channel as it crosses the ridge. These results suggest that there is a significant amount of deformation ongoing within the High Moma Range, several tens of kilometers inward from the deformational front, the MTF. The Taskan Ridge is ~20 km south of the topographic front of the eastern Moma Range, where Gaiduk et al. (1993) have extended the ITT. Many of the structures mapped in the Arga-Tas mountains are poorly constrained by field observation, so my interpretations of the geomorphic indicators should be treated as a preliminary conjecture.

The spatial distribution of k_{sn} values in the Moma Range is not totally clear, but higher values appear concentrated the central portions of the Moma Range, centered around the vicinity of the Myatis River and the Ilin'-Tas Mountains (Fig. 21). I interpret this as a result of long-term (10 kyr to 300 kyr) sustained uplift rates in this location. In addition, streams sourced from the High Moma Range, south of ITT, have higher k_{sn} values assigned to their profiles; while streams sourced north of the fault, in the northern foothills, have lower k_{sn} values. These changes from

high to low channel steepness could be an implication that uplift rates from south to north are broken by a distinct structural boundary. An alternative interpretation is that uplift rates are gradational from high to low elevations. The geomorphic indicators, particularly the narrowed channel segments on the Myatis and Kyllakh rivers (Fig. 14), corroborate the notion that ITT represents a boundary between high and low uplift regimes across the Moma Range, in turn suggesting that portions of the fold-and-thrust belt are subject to out-of-sequence deformation.

6.2 Earthquakes in the Moma Range

Seismological studies in northeast Russia (e.g., Parfenov et al., 1988; Cook et al., 1986; Fujita et al., 2009) and in many other tectonic plate boundary regions, use earthquakes as a major strain indicator along plate boundaries or plate boundary zones. Over fifty events have been recorded in the Moma Range fold-and-thrust belt, but most of the events are smaller than mb 3.0 (Fujita et al., 2009; Mackey et al., 2010). Only a few events have exceed m_b 4.0: one m_b 5.0 in Ilin'-Tas Mountains (144°, 67°; Figs. 21 and 24), two m_b 4.0 events in eastern foothills of the Arga-Tas Mountains, and three large events distributed within western foothills of the Andrei-Tas Mountains, with moment magnitudes (M_w) 6.6, 6.1 and 5.3 (Figs. 23 and 24). The geomorphic indicators that coincide with the active out-of-sequence thrust structures (i.e. the ITT), are loosely coupled with any sort of seismicity. But epicenters and depth estimates of individual events are limited by the seismic network currently in place in northeast Russia, and thus are poorly constrained. In addition to this, many of these events likely occur along thrust ramps in the shallow (< 15 km) sedimentary cover, hindering the use of teleseismic data to obtain reliable epicenters and magnitudes (Jackson, 1980).

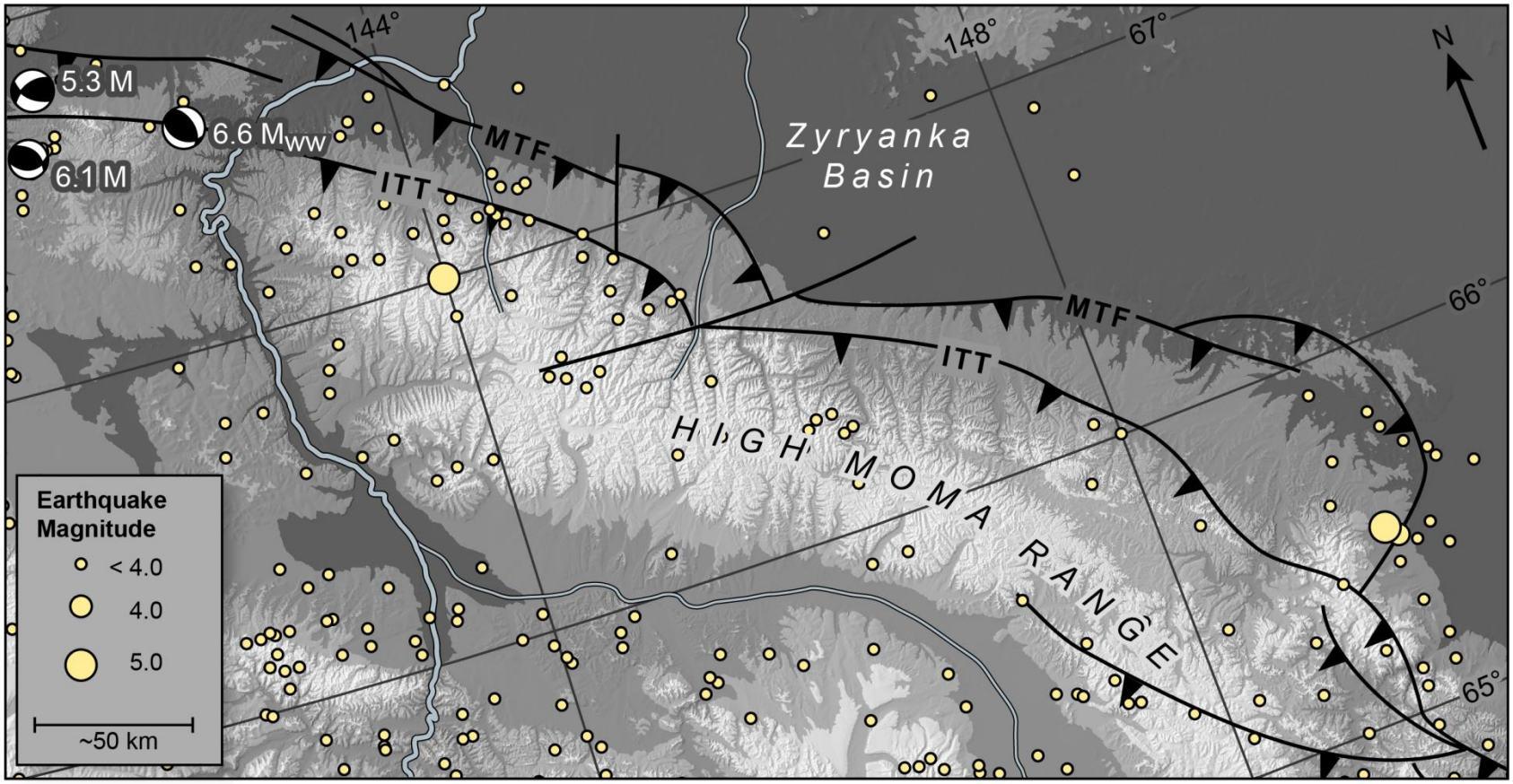

Figure 24. Seismicity map of the Moma Range fold-and-thrust belt. Focal mechanisms are shown with their corresponding magnitudes. M_{WW} 6.6 is the February 14, 2013 event.

The magnitude of shallow seismic events in thrust ramps from fold-and-thrust belts can range between moderate to large ($5.0 < M_w < 7.5$) (Namson and Davis, 1990), and their distribution and magnitude are thought to be strongly controlled by basal friction along a decollement (Koyi et al., 2000). Only three events of moderate to large magnitude have been recorded teleseismicly in the Moma Range, the three large events in the Andrei-Tas Mountains, all have compressional moment tensor solutions (Figs. 23 and 24). This could indicate that this portion of the fold-and-thrust belt is accommodating more of the convergence, that it is the most currently active portion, or that it could be related to lateral differences in decollement strength. Koyi et al. (2000) demonstrated that fold-and-thrust belts shortened above a frictional decollement tend to have larger magnitude earthquakes that take place along short-lived thrust ramps within narrow seismic zones. A frictional decollement is realistic for the Moma Range, as rocks that constitute weak decollements, rock salt and mudstone, are absent from the regional stratigraphy. Slip along thrust ramps connected to a frictional decollement might explain why the large earthquakes occur in a focused area (Andrei-Tas Mountains). The structures in the central and eastern portions of the fold-and-thrust belt may have been short lived, during a time before instrumental seismology, but active in the very recent geologic past (<10 kyr). This could explain why the ITT in the central and eastern portions of the Moma Range has a strong geomorphic signal, but is absent of large-magnitude earthquakes. This would suggest that the earthquake recurrence rate is slow and that the eastern portions of the Moma Range have not ruptured within instrumental seismology timeframe.

Alternatively, the differences in epicenter distribution across the fold-and-thrust belt are possibly related to the lateral changes in decollement strength. In this case, the western portion has the larger-magnitude earthquakes because it is deforming above a frictional decollement.

Conversely, the central and eastern portions of the fold-and-thrust belt lack large-magnitude earthquakes and appear to be deforming out-of-sequence/internally. Out-of-sequence thrusting is known to be maintained in fold-and-thrust belts deforming above weak decollements (Koyi et al., 2000). In this scenario, active displacement along both the major bounding faults of the trust zone, ITT and MTF, would be expected and possibly taking place aseismically. More detailed stratigraphic and geophysical studies that target the nature and characteristics of the decollement below the thrust ramps of Moma Range are needed to test these models.

6.3 Mechanisms for out-of-sequence deformation

No mechanistic model currently exists to explain the occurrence of active thrusting in the Moma Range fold-and-thrust belt, so the material discussed here is preliminary and speculative. I apply the critical taper theory proposed by Davis et al. (1983) where the deformation of the Moma Range is comparable to that of a Coulomb wedge (e.g., a sand wedge) pushed by a backstop. In the early stages of development, during collision between the Siberian Craton and the Kolyma–Omolon superterrane, the wedge (i.e., the sedimentary cover referred to as the Ilin'-Tas assemblage) deforms internally by forming a complex series of folds, the Ilin'-Tas Anticlinorium (Parfenov, 1991). As a consequence of folding, the wedge increases its surface slope until it reaches a certain critical taper (the surface slope angle plus the dip of the decollement). Internal friction builds up in the wedge and it overcomes the coefficient of friction along the decollement, and the wedge slides forward as a whole forming frontal thrust at the outer edge. This is probably what happened during Cretaceous to early Cenozoic deformation of the Moma Range (Prokopiev, 2000; Fridovsky and Prokopiev, 2002). What occurs after this stage in the Moma Range remains unknown.

Gaiduk et al. (1993) showed that the frontal thrust, the MTF, displaces the Early Cretaceous Zyryanka Series on top of the Eocene to Miocene Myatis Series (Fig. 5). Many of the Russian authors (e.g., Ivanov, 1985; Grinenko et al., 1999) cap the thrusting under a Late Miocene and Pliocene unconformity that is found at the base of the Kyllakh formation (Fig. 5), but convincing field evidence that shows truncation of the thrust by the unconformity is missing. One interpretation is the sediments of the Kyllakh formation were deposited in the form syntectonic strata in front and on top of the growing Zyryanka thrust zone.

Results from this study show that the central and eastern portions of the fold-and-thrust belt are currently (or very recently) deforming out-of-sequence. Davis et al. (1983) demonstrated that out-of-sequence deformation occurs as a consequence of decreasing the surface slope of the Coulomb wedge, typically by means of erosion. However, out-of-sequence deformation is now common in many fold-and-thrust belts, and is not exclusively linked to erosion. Conditions such as weak decollements (Koyi et al., 2000; Nieuwland et al., 2000), syntectonic sedimentation (Storti and McClay, 1995), and extensional collapse (Willett, 1992) can all decrease the surface slope the deforming wedge, in turn causing out-of-sequence thrusting.

In the case of the Moma Range, the surface slope of the wedge was possibly lowered below its critical taper during the Late Eocene to early Pliocene. At this time, convergence between the North American, Eurasian, and Okhotsk plates reached a standstill, potentially caused by the southward migration of the NA–EU pole of rotation as proposed by several authors (e.g., Cook et al., 1986; Parfenov, 1988; Fujita et al., 1990; Merkouriev and DeMets, 2008). This would have been coupled with removal of wedge material by erosion, decreasing the surface slope angle. The repositioning of the rotation pole to its current northern location, has

reinitiated convergence in the region, triggering crustal shortening that is accommodated in the wedge's interior (the High Moma Range) by out-of-sequence deformation.

Out-of-sequence deformation in the north slope of Moma Range has not previously been suggested, but the results of my geomorphologic analysis are similar to those recently reported in studies of out-of-sequence thrusting in the Himalayan fold-and-thrust belt. Contrary to the traditional model of deformation in the Himalaya, Wobus et al., (2003, 2005, 2006) invoke a locus of active deformation well north (~100 km) of the traditional deformation front, the Main Frontal Thrust. Their findings are based on knickpoints observed in stream profiles (Wobus et al., 2003, 2006), field mapping of deformational and geomorphic features (Hodges et al., 2004), discontinuities in thermochronologic data (Wobus et al., 2003), and elevated erosion rates (Wobus et al., 2005). The zone of deformation proposed by these authors coincides with a strong precipitation gradient, presumably triggering a narrow zone of enhanced erosion, and thus a dynamic feedback relationship between climate and tectonics (Wobus et al., 2003, 2005; Hodges et al., 2004).

An alternative analog for the out-of-sequence thrusting in the Moma Range is the Zagros fold-and-thrust belt in Iran. There, the out-of-sequence thrusting is controlled by lateral differences in decollement strength that separate the northwestern and southeastern portions of the fold-and-thrust belt (Koyi et al., 2000 and references therein). In the northwest part of the Zagros (strong decollement) the epicenters of moderate to large-magnitude earthquakes occur within a narrow zone, along thrust ramps at the outer edge of the fold-and-thrust belt (Koyi et al., 2000). In the southeast (weak decollement), the earthquakes are spread out over a broad zone, and the large-magnitude earthquakes are restricted to displacements along the deep-seated basement faults (Ni and Barazangi, 1986; Jackson and McKenzie, 1984).

The out-of-sequence deformation in the Moma Range fold-and-thrust belt differs from that of the Himalaya and the Zagros because it is possibly linked to a complex middle Cenozoic history, where the regional convergence has been switched on and off. There appears to be no dynamic feedback between climate and tectonics, and variations in decollement strength are speculative at this time, although neither scenario should be ruled out. The Cenozic evolution of the Moma Range fold-and-thrust belt, is complicated by the potential existence of a continental rifting event, the Moma Rift (e.g., Grachev, 1982; Fujita et al., 1990; Franke et al., 2000; Tschegg et al., 2011). The evidence supporting the Moma Rift is the series of topographical and structural depressions (e.g., the Moma-Selennyakh depression, Fig. 3) that trend northwest-southeast behind the Moma Range. In addition to the surface expression of the rift, is the presence of the hot springs (Grachev, 1982), Cenozoic volcanism (Tschegg et al., 2011), elevated heat flow measurements (Duschkov and Sokolova, 1985), and regionally lower crustal thickness (Parfenov, 1988; Mackey et al., 1998). While Russian authors originally argued for a modern continuation of the Gakkel Ridge from the Arctic into and actively rifting Asian continent, many authors have confirmed that rifting was aborted in the Pliocene, when extensional forces changed to compression (e.g., Cook et al., 1986; Parfenov et al., 1988; Fujita et al., 1990; Franke et al., 2000). Tschegg et al. (2011) obtained six $^{40}Ar/^{39}Ar$ plateau ages from the Rudich basanites (volcanic rocks commonly associated with continental rifting) that yield ages ranging from 36.0 ± 0.8 to 38.3 ± 0.6 Ma (middle Eocene). They conclude that the extrusion of the Rudich basanites possibly represents the onset of continental rifting and the continuation of Gakkel Ridge extension into the Asian continent. However, there is a discrepancy between onset of volcanism (middle Eocene, Tschegg et al., 2011) and the presumed southward migration of the NA-EU rotation pole (middle Miocene, e.g., Merkouriev and DeMets, 2008). Regardless of this

discrepancy, continental extension, via rifting, likely had a profound effect on the thickness of the wedge (i.e., the Moma Range fold-and-thrust belt).

With the slow convergence rates (<10 mm/yr) between North America and Eurasia in the region, it might take millions of years for the fold-and-thrust belt to build up enough internal deformation to regain its critical taper, and resume the break-forward sequence, where slip displacement is focused on thrust ramps at the outer edge of the of the fold-and-thrust belt (i.e., along the MTF or faults further out in the foreland). This is not to say that all portions of the Moma Range are currently deforming internally, but that there might be lateral variations in where the deformation takes place. In the foothills of the Andrei-Tas Mountains, the large-magnitude earthquakes are probably occurring because of displacement along a frontal thrust ramp equivalent to the MTF. The epicenters of those earthquakes do coincide with a topographic front and possible westward continuation of the ITT (Fig. 24); however, with the depth of these events (~10 km) factored in, they are likely associated with structures that meet the surface far out in the foreland. But the results presented in this study should not be ignored. There is clearly a connection between the geomorphic indicators and the very recent displacements in the central portions of the fold-and-thrust belt along ITT, an out-of-sequence thrust fault. These contrasting styles of deformation along-strike could be attributed to number of limiting factors (e.g., original wedge thickness, variations in decollement strength, erosion patterns, syntectonic sedimentation), but without further geological and geophysical data, many of these questions will remain unanswered.

6.4 Limitations of the analysis

There are two primary issues that limit the reliability of this study: the resolution of the raw data (topography and satellite imagery), and the shortage of ground-truthing geological and

geophysical data. The resolution of the topographic and the satellite data limits how much detail can be retained in the geomorphic analysis. Knickpoints and changes in channel morphology might go totally unnoticed. The largest deficiency in the raw data is the low resolution of the topographic maps that the DEM was constructed from. They are currently mapped at 1:200,000 with a 40 m contour interval. This means that there is roughly 130 ft. between contour lines, a vertical distance represented by thirteen contours on the 1:24,000 topographic maps of the contiguous US. Higher resolution elevation data with global coverage has become more readily available to the public in past couple of years, in particular, the ASTER Global Digital Elevation Model (http://www.jspacesystems.or.jp/ersdac/GDEM/E/index.html). It provides a 30 m resolution for nearly the entire globe, but using this data requires additional processing to fix the anomalies and artifacts within the raw data. Increasing the spatial resolution of the elevation data will greatly enhance future remote sensing research in northeast Russia.

There are still a few unknowns associated with the channel steepness index (k_{sn}). The largest assumption made is that K, the erosion coefficient from equation 2, is uniform throughout the Moma Range, and that k_{sn} is a direct consequence of rock uplift rates. However, Duvall et al. (2004) noticed from their field site in coastal California, that rock uplift rates vary between ~.75 and ~5 mm yr^{-1}, a six- to seven-fold difference, but only a twofold differences in k_{sn} values were observed (~13.8 to ~26.1). They suggest this ambiguity is the result of a channel's tendency to narrow its width with increased rock uplift, and thus changing the K with respect to rock uplift. For this reason, I looked for narrowed channel segments as the rivers crossed the major faults, and with a better satellite image resolution (or access to aerial photographs) more narrowed channel segments might be visible.

The biggest challenge in using remote sensing in a poorly studied, tectonically active region like northeast Russia, is the difficulty in ground-truthing the observations derived from the remotely sensed data with geological and geophysical data. For example, the erosion coefficients, K, discussed in the last paragraph are poorly constrained because no data exist on the strength of channel bed lithology. With no fieldwork to the region, I cannot confirm whether the changes stream behavior (e.g., channel steepness, knickpoints, or channel morphology) are truly a function of rock uplift or channel bed lithology. Furthermore, detailed the geological data are only available for a very small area within the fold-and-thrust belt, primarily in the Myatis River region (Gaiduk and Prokopiev, 1999). Having the opportunity to go in the field and map faults and potential shear zones within the fold-and-thrust belt would constrain some of the uncertainties associated with the geomorphic indicators and improve the mechanistic model presented in this research.

The last of the major limitations are uncertainties in the subsurface of the Zyryanka foredeep. Very few wells have been drilled there and even fewer seismic lines cross it. Regardless, none of the subsurface data is yet available to western scientists. Much of what is known about the foredeep is derived from gravity surveys (Parfenov, 1988), but these data are out of date and of poor resolution. A geomorphic approach to finding active structures only records processes that occur on the surface. There may be active structures that are buried beneath the alluvial plane of the foreland, but without the ability to image such structures and their exclusion from the geomorphic analysis, forces them to remain unaccounted for.

6.5 Future Research

Future research needs to be field focused. One approach to resolve some of the problems presented in this research would be to conduct a low-temperature thermochronology transect

across the fold-and-thrust belt. By sampling within the individual thrust sheets and applying $^{40}Ar/^{39}Ar$, fission track and (U-Th)/He techniques to the minerals found within the sedimentary rocks, the timing and rates of uplift associated with the growth of the Moma Range could be established, thus verifying or repudiating the results from this preliminary study. Fieldwork would also afford the opportunity to map out the major thrust structures and help establish a better structural framework for the Moma Range fold-and-thrust belt.

7. CONCLUSIONS

The results from this research suggest that the Moma Range is an actively growing fold-and-thrust belt that accommodates some convergence between North America, Eurasia, and Okhotsk. Uplift of the fold-and-thrust began in the Late Cretaceous, after the closure of the Oimyakon Ocean and the onset of the Verkhoyansk-Kolyma Orogen (VKO) (Parfenov, 1991). Uncertainties remain about the fold-and-thrust belt's Cenozoic history, but convergence presumably paused during a middle Cenozoic continental rifting episode, the Moma Rift (e.g., Tschegg et al., 2011). The northward migration of the North American—Eurasian pole of rotation (Cook et al., 1986), reestablished thrusting in the Moma Range during the Pliocene (Gaiduk et al., 1993).

In an analysis of DEM and satellite data, I studied the geomorphic expression of the rivers that drain the northeast slope of the Moma Range in an attempt to identify active thrust faults to establish a structural framework for the fold-and-thrust belt. There are three main take home points from this research:

1. Portions of the fold-and-thrust belt are deforming internally or out-of-sequence. The Indigirka's abrupt change in channel sinuosity, as it cuts across the Moma Range, suggests broad internal folding and uplift. This out-sequence deformation extends over to the central portions of the fold-and-thrust belt, in the Ilin'-Tas Mountains (Fig. 3), where thrusting is maintained at the topographic front of the High Moma Range, along Ilin'-Tas thrust fault (ITT). High-order streams that cross the ITT here experience significant channel narrowing, and streams that are sourced above the ITT tend to have steepened profiles. In the eastern portions of the fold-and-thrust belt, near the Arga-Tas Mountains, deformation is possibly focused along the Taskan

Ridge, a structure situated within the hinterland of the fold-and-thrust belt (~20 km south of ITT). The ITT has a strong geomorphic expression in the Andrei-Tas Mountains, but the recent earthquakes in the region suggest that thrusting is probably maintained out in front of the fold-and-thrust belt there.

2. Styles of deformation vary along strike of fold-and-thrust belt. Uplift rates, inferred from the normalized steepness values (k_{sn}), appear to not be spatial uniform along the fold-and-thrust belt, but concentrated in certain localities. The heightened k_{sn} values in the Ilin'-Tas Mountains suggests sustained uplift rates over longer timescales (10 kyr to 300 kyr). Additionally, the recorded seismicity varies along strike of the fold-and-thrust belt. All of the large-magnitude thrust events have epicenters in the Andei-Tas Mountains, and this corresponds with a general west to east decrease in seismicity along the fold-and-thrust belt.

3. Remote sensing can be used to obtaining meaningful information on the tectonics of an inaccessible region like northeast Russia, but it needs complementary data. Without earthquakes or previously mapped faults, the components of this research would remain largely inconclusive. The tools used in analyzing stream profiles are still in their early stages of development, and without higher resolution of elevation and satellite data in the Moma Range, the analysis is limited to first-order observations; however, the results from this research provide a useful reconnaissance for future field investigation.

A unified, mechanistic model that explains the out-of-sequence thrusting and the along-strike variation in the fold-and-thrust belt remains incomplete. Complexities in these models are

probably associated with the rather rapid changes in the tectonic environment the region underwent during the middle Cenozoic, but are also likely influenced by additional factors (such as decollement strength or syntectonic sedimentation). These models await further field study, additional seismic monitoring, and expanded geophysical surveys to more precisely map out the active structures and to construct a more complete structural framework for the Moma Range fold-and-thrust belt.

REFERENCES

REFERENCES

Amos, C. B., and Burbank, D. W., 2007, Channel width response to differential uplift: Journal of Geophysical Research, v. 112, F02010, doi:10.1029/2006JF000672.

Alexander, J., Bridge, J. S., Leeder, M. R., Collier, R. E. L., and Gawthorpe, R. L., 1994, Holocene meander-belt evolution in an active extensional basin, southwestern Montana: Journal of Sedimentary Research, v. 64, p. 542-559.

Barka, A. A. (1992). The north Anatolian fault zone: In *Annales Tectonicae* v. 6, p. 164-195.

Bird, P., 2003, An updated digital model of plate boundaries: Geochemistry, Geophysics, Geosystems, v. 4, p. 1027, doi: 10.1029/2001GC000252.

Bullard, T.F. and Lettis, W.R., 1993, Quaternary fold deformation associated with blind thrust faulting, Los Angeles Basin: California. Journal of Geophysical Research, v. 98, p. 8349-8369.

Calais, E., DeMets, C., and Nocquet, J. M., 2003, Evidence for a post-3.16-Ma change in Nubia–Eurasia–North America plate motions?: Earth and Planetary Science Letters, v. 216, p. 81-92.

Cawood, P. A., Kröner, A., Collins W. J., Kusky, T. M., Mooney, W. D., Windley B.F., 2009, Accretionary orogens through Earth history, *in* Cawood, P.A., and Kröner, A., eds., Earth Accretionary Systems in Space and Time: Geological Society of London Special Publication 318, p. 1–36.

Chapman, M. E. and Solomon, S. C., 1976, North American –Eurasian plate boundary in northeast Asia: Journal of Geophysical Research, v. 81, p. 921–930.

Cook, D. B., Fujita, K., and McMullen, C. A., 1986, Present-day plate interactions in northeast Asia: North American, Eurasian, and Okhotsk plates: Journal of Geodynamics, v. 6, p. 33–51.

Cyr, A. J., Granger, D. E., Olivetti, V., and Molin, P., 2010, Quantifying rock uplift rates using channel steepness and cosmogenic nuclide–determined erosion rates: Examples from northern and southern Italy: Lithosphere, v. 2, p. 188-198, **doi: 10.1130/L96.1**

Davis, D., Suppe, J., and Dahlen, F. A., 1983, Mechanics of fold-and-thrust belts and accretionary wedges: Journal of Geophysical research, v. 88, p. 1153-1172.

DeMets, C., Gordon, R.G., Argus, D.F. and Stein, S., 1990, Current plate motions, Geophysical Journal International, v. 101, p. 425–478, doi: 10.1111/j.1365-246X.1990.tb06579.x.

DeCelles, P. G., and Giles, K. A, 1996, Foreland basin systems: Basin Research, v. 8, p. 105-123, doi: 10.1046/j.1365-2117.1996.01491.x

Digital elevation data (63 m), 2009., de Ferranti, J., Retrived from www.viewfinderpanoramas.org

Duchkov A.D. and Sokolova, L.S., 1985, Temperature of the lithosphere of Siberia according to geothermal data: Soviet Geology and Geophysics, v. 26, p. 53–61. (in Russian)

Duvall, A., Kirby, E., and Burbank, D., 2004, Tectonic and lithologic controls on bedrock channel profiles and processes in coastal California: Journal of Geophysical Research, v. 109, F03002, doi:10.1029/2003JF000086.

England, P. and Jackson, J., 1989, Active deformation in the continents: Annual Reviews of Earth and Planetary Sciences, v. 17, p. 197–226.

Fridovsky, V. Y., and Prokopiev, A. V., 2002, Tectonics, geodynamics and gold mineralization of the eastern margin of the North Asia craton, *in* Blundell, D.J., Neubauer, F., and von Quadt, a., eds., The timing and location of major ore deposits in an evolving orogen: Geological Society, London, Special Publications, v. 204, p. 299-317. doi:10.1144/GSL.SP.2002.204.01.17

Fujita, K., and Newberry, J. T. 1982, Tectonic evolution of northeastern Siberia and adjacent regions: Tectonophysics, v. 89, p. 337-357.

Fujita, K., Cambray, F. W., and Velbel, M. A., 1990, Tectonics of the Laptev Sea and Moma rift systems, northeastern USSR: Marine Geology, v. 93, p. 95–118.

Fujita, K., Stone, D., Layer, P., Parfenov, L., and Kozmin, B., 1997 Cooperative program helps decipher tectonics of Northeastern Russia: Eos (Transactions, American Geophysical Union), v. 78, p. 252-253.

Fujita, K., Kozmin, B., Mackey, K., Riegel, S., Imaev, V., and McLean, M., 2009, Seismotectonics of the Chersky seismic belt, eastern Sakha Republic (Yakutia) and Magadan district, Russia: Stephan Mueller Special Publication Series, v. 4, p. 117-145.

Gaiduk, V.V., Syundyukov, I.Sh., Grinenko, O.V., and Imaev, V.S., 1989, The structure and petroleum potential of the Cenozoic Indigirka–Zyryanka basin, in: Tectonics and Petroleum Potential of Yakutia. YaNTs SO AN SSSR, Yakutsk, pp. 75–87 (in Russian).

Gaiduk, V.V., Grinenko, O. V., Imaev, V.S., 1990, Late Cenozoic folding of the Ilin'-Tas anticlinorium (Verkhoyansk-Kolyma fold system): Doklady Earth Sciences, v. 312, p. 431-434 (in Russian).

Gaiduk, V. V., Grinenko, O. V., and Syundyukov, I. S., 1993, The age of the folding in the Moma-Zyryanka basin: Tikhookean. Geol., v. 3, p. 99–108 (in Russian).

Gaiduk, V. V. and Prokopiev, A. V., Research methods in fold-and-thrust belts: Nauka, Novosibirsk, 1999 (in Russian).

Gaina, C., Roest, W. R., and Müller, R. D., 2002, Late Cretaceous–Cenozoic deformation of northeast Asia: Earth and Planetary Science Letters, v. 197, p. 273-286.

Gardner, T. W., 1983, Experimental study of knickpoint and longitudinal profile evolution in cohesive, homogeneous material: Geological Society of America Bulletin, v. 94, p. 664-672.

Gordon, R. G., 1998, The plate tectonic approximation: Plate nonrigidity, diffuse plate boundaries, and global plate reconstructions: Annual Review of Earth and Planetary Sciences, v. 26, p. 615-642.

Grinenko, O. V., Sergeenko, A. I., and Belolyubskij, I. N., 1999, Lower Palaeocene of the Moma-Zyryanka basin: Otechestvennaya geologiya, v. 4, p. 35-37 (in Russian).

Hack, J.T., 1957, Studies of Longitudinal Profiles in Virginia and Maryland: U. S. Geological Survey Professional Paper 294-B, p. 45–97.

Hack, J.T., 1973, Stream profile analysis and stream-gradient index: U.S. Geological Survey Journal of Research, v. 1, p. 421-429.

Hindle, D., Fujita, K., and Mackey, K., 2006, Current deformation rates and extrusion of the northwestern Okhotsk plate, northeast Russia: Geophysical Research Letters, v. 33, L02306, doi:10.1029/2005GL024814.

Hindle, D., Fujita, K., and Mackey, K., 2009, Deformation of the Northwestern Okhotsk Plate: How is it happening?: Stephan Mueller Special Publication Series, v. 4, p. 147-156.

Hindle, D., and Mackey, K., 2011, Earthquake recurrence and magnitude and seismic deformation of the northwestern Okhotsk plate, northeast Russia, Journal of Geophysical Research, v. 116, B02301,

Hodges, K. V., Wobus, C., Ruhl, K., Schildgen, T., and Whipple, K., 2004, Quaternary deformation, river steepening, and heavy precipitation at the front of the Higher Himalayan ranges: Earth and Planetary Science Letters, v. 220, 379-389.

Howard, A.D., Dietrich, W.E., and Seidl, M.A., 1994, Modeling fluvial erosion on regional to continental scales: Journal of Geophysical Research, v. 99, p. 13971–13986.

Howard, A.D., 1994, A detachment-limited model of drainage basin evolution: Water Resources Research, v. 30, p. 2261–2285

Hu, X. and Pollard, W. H., 1997, The Hydrologic Analysis and Modelling of River Icing Growth, North Fork Pass, Yukon Territory, Canada: Permafrost and Periglacial Processes, v. 8, p. 279–294, doi: 10.1002/(SICI)1099-1530(199709)8:3<279::AID-PPP260>3.0.CO;2-7

Imaev, V. S., 1991, Late Cenozoic overthrusts, reverse faults and folded dislocations of the Chersky seismic belt (eastern Yakutia), Geotectonics, vol. 25, p. 356–361.

Imaev, V. S., Imaeva, L. P., and Koz'min, B. M.: Active Faults and Seismotectonics of Northeast Yakutia, Yakutskii Nauchnyi Tsentr SO AN SSSR, Yakutsk, 1990 (in Russian).

Imaev, V. S., Imaeva, L. P., Koz'min, B. M., and Fujita, K., 1994 Active faults and recent geodynamics of Yakutian seismic belts, Geotectonics, vol. 28, p. 146–158.

Imaev, V. S., Imaeva, L. P., and Koz'min, B. M., 1995, Seismotectonic dislocations in seismic belts of Yakutia, Geotectonics, vol. 29, p. 73–86.

Ivanov, V.V 1985, Sedimentary basins of northeast Asia: Petroleum Geology, v. 22, p. 234-296

Jackson, J., 1980, Errors in focal depth determination and the depth of seismicity in Iran and Turkey: Geophysical Journal of the Royal Astronomical Society, v. 61, p. 285-301.

Jackson, J., and McKenzie D. P., 1984, Active tectonics of the Alpine-Himalayan Belt between western Turkey and Pakistan: Geophysical Journal of the Royal Astronomical Society, v. 77, p. 185-264.

Jackson, J., Norris, R., and Youngson, J., 1996, The structural evolution of active fault and fold systems in central Otago, New Zealand: Evidence revealed by drainage patterns: Journal of Structural Geology, v. 18, p. 217-234.

Kirby, E., and Whipple, K., 2001, Quantifying differential rock-uplift rates via stream profile analysis. Geology, v. 29, p. 415-418.

Kirby, E., Whipple, K.X., Tang, W., and Chen, Z., 2003, Distribution of active rock uplift along the eastern margin of the Tibetan Plateau: Inferences from bedrock channel longitudinal profiles: Journal of Geophysical Research, v. 108, 2217, doi: 10.1029/2001JB000861.

Kogan, M. G., Steblov, G. M., King, R. W., Herring, T. A., Frolov, D. I., Egorov, S. G., Levin, V. Y., Lerner-Lam, A., and Jones, A., 2000, Geodetic constraints on the rigidity and relative motion of Eurasia and North America, Geophysical Research Letters, vol. 27, p. 2041–2044.

Kolpakov, V.V., 1986. National geologic map of USSR (new series). Map of Quaternary deposits, Q-54, 55 (Khonuu). Scale, 1:1,000,000. VSEGEI, Leningrad (in Russian).

Koyi, H.A., Hessami, K., and Teixell, A., 2000, Epicenter distribution and magnitude of earthquakes in foldthrust belts: Insights from sandbox models: Geophysical Research Letters, v. 27, no. 2, p. 273–276, doi: 10.1029/1999GL010833.

Koz'min, B. M., 1984. Seismic belts of Yakutia and their earthquake focal mechanisms, Nauka, M., 127 pp. (in Russian).

Layer, P. W., Newberry, R., Fujita, K., Parfenov, L., Trunilina, V., and Bakharev, A., 2001, Tectonic setting of the plutonic belts of Yakutia, northeast Russia, based on 40Ar/39Ar geochronology and trace element geochemistry: Geology, v. 29, p. 167-170.

Lesh, M.E., and Ridgway, K.D., 2007, Geomorphic evidence of active transpressional deformation in the Tanana foreland basin, south-central Alaska, in Ridgway, K.D., Trop, J.M., Glen, J.M.G., and O'Neill, J.M., eds., Tectonic Growth of a Collisional Continental Margin: Crustal Evolution of Southern Alaska: Geological Society of America Special Paper, v. 431, p. 573-592,

Mackey, K. G., Fujita, K., and Ruff, L. J., 1998, Crustal thickness of northeast Russia: Tectonophysics, v. 284, p. 283-297.

Marple, R. T., and Talwani, P., 1993, Evidence of possible tectonic upwarping along the South Carolina coastal plain from an examination of river morphology and elevation data: Geology, v. 21, p. 651-654.

McKenzie, D. 1972, Active tectonics of the Mediterranean region: Geophysical Journal of the Royal Astronomical Society, v. 30, p. 109-185

Merritts, D.J., Vincent, KR, and Wohl, E.E., 1994, Long river profiles, tectonism, and eustasy: A guide to interpreting fluvial terraces: Journal of Geophysical Research, v. 99, p. 14,031-14,050.

Merkouriev, S., and DeMets, C., 2008, A high-resolution model for Eurasia–North America plate kinematics since 20 Ma: Geophysical Journal International, v.173, p. 1064-1083.
Milliman, J. D., and Syvitski, J. P., 1992, Geomorphic/tectonic control of sediment discharge to the ocean: the importance of small mountainous rivers: The Journal of Geology, v. 100, p. 525-544.

Montgomery, D.R., and Foufoula-Georgiou, E., 1993, Channel network source representation using digital elevation models: Water Resources Research, v. 29, p. 1178–1191.

Morgan, W. J., 1968, Rises, trenches, great faults, and crustal blocks: Journal of Geophysical Research, v. 73, p. 1959-1982.

Namson, J., and Davis, T. L., 1990, Late Cenozoic fold and thrust belt of the southern Coast Ranges and Santa Maria basin, California: American Association of Petroleum Geologists Bulletin, v. 74, p. 467-492.

Ni, J., and Barazangi M. J., 1986, Seismotectonics of the Zagros continental collision zone and a comparison with the Himalayas: Journal of Geophysical Research, v. 91, p. 8205-8218.

Nieuwland, D. A., Leutscher, J. H., and Gast, J., 2000. Wedge equilibrium in fold-and-thrust belts: prediction of out-of-sequence thrusting based on sandbox experiments and natural examples: *Geologie en Mijnbouw*, v. *79*, p. 81-92.

Ouchi, S., 1985, Response of alluvial rivers to slow active tectonic movement: Geological Society of America Bulletin, v. 96, p. 504-515.

Oxman, V. S., Parfenov, L. M., Prokopiev, A. V., Timofeev, V. F., Tretyakov, F. F., Nedosekin, Y. D., Layer, P.W., and Fujita, K., 1995, The Chersky range ophiolite belt, northeast Russia: The Journal of Geology, v. 103, p. 539-557.

Peach, H. J., 2009, Geotectonic setting of the Teriary Uyandina and Indigirka-Zyryanka basins, Republic Sakha (Yakutia), Northeast Russia, using coal rank data: Stephan Mueller Special Publication Series, v. 4, p. 85–96.

Parfenov, L. M., Koz'min, B. M., Grinenko, O. V., Imaev, V. S., and Imaeva, L. P., 1988, Geodynamics of the Chersky seismic belt: Journal of Geodynamics, v. 9, p. 15–37.

Parfenov, L.M., 1991, Tectonics of the Verkhoyansk-Kolyma Mesozoides in the context of plate tectonics: Tectonophysics, v. 199, p. 319–342.

Ponza, A., Pazzaglia, F. J., and Picotti, V., 2010, Thrust-fold activity at the mountain front of the Northern Apennines (Italy) from quantitative landscape analysis: Geomorphology, v. 123, p. 211-231.

Prokopiev, A. V., 2000, Verkhoyansk–Chersky collisional orogen: Geology of the Pacific Ocean, v. 15, p. 891-904.

Riegel, S. A., Fujita, K., Koz'min, B. M., Imaev, V. S., and Cook, D. B., 1993, Extrusion tectonics of the Okhotsk plate, northeast Asia: Geophysical Research Letters, v. 20, p. 607–610.

Roe, G.H., Montgomery, D.R., Hallet, B., 2002, Effects of orographic precipitation variations on the concavity of steady-state river profiles: Geology, v. 30, p. 143–146.

Savostin, L. A. and Karasik, A. M., 1981, Recent plate tectonics of the Arctic basin and of northeastern Asia: Tectonophysics, v. 74, p. 111–145.

Savostin, L.A, Zonenshain, L., and Baranov, B., 1983, Geology and plate tectonics of the Sea of Okhotsk: American Geophysical Union Geodynamics Series, v. 11, p. 189–221.

Savostin L.A., Karasik, A.M. and Zonenshain, L.P., 1984, The history of the opening of the Eurasia basin in the Arctic. Translation, USSR Academy of Science, Earth Science Sector, v. 276, p.79-83

Seno, T., Sakurai, T., and Stein, S., 1996, Can the Okhotsk plate be discriminated from the North American Plate?: Journal of Geophysical Research, v. 101, p. 11,305–11,315.

Sella, G. F., Dixon, T. H., and Mao, A., 2002, REVEL: A model for Recent plate velocities from space geodesy: Journal of Geophysical Research, v. 107, p. 2081

Schumm, S. A., 1986, Alluvial river response to active tectonics: Active tectonics, p. 80-94, National Academic press, Wasington, D.C.

Snow, J.E., and Edmonds, H.N., 2007, Ultraslow-spreading ridges: Rapid paradigm changes: Oceanography v. 20, p. 90–101

Sklar, L., and Dietrich,W.E., 1998, River longitudinal profiles and bedrock incision models: Stream power and the influence of sediment supply, *in* Tinkler, K.J., and Wohl, E.E., eds., Rivers over rock: Fluvial processes in bedrock channels: American Geophysical Union Geophysical Monograph 107, p. 237–260.

Snyder, N. P., Whipple, K. X., Tucker, G. E., and Merritts, D. J., 2000, Landscape response to tectonic forcing: Digital elevation model analysis of stream profiles in the Mendocino triple junction region, northern California: Geological Society of America Bulletin, v. 112(8), p. 1250-1263.

Storti, F., and McClay, K., 1995, Influence of syntectonic sedimentation on thrust wedges in analogue models: Geology, v. 23, p. 999-1002.

Surmilova, E.P., Maksimova, G.A. and Natapov, L.M., 1986, National geologic map of the USSR (new series), map of pre-Quarternary formations, Q-54, 55 (Khonuu) Scale, 1:1,000,000, VSEGEI, Leningrad (in Russian).

Tschegg, C., Bizimis, M., Schneider, D., Akinin, V. V., and Ntaflos, T., 2011, Magmatism at the Eurasian–North American modern plate boundary: Constraints from alkaline volcanism in the Chersky Belt (Yakutia): Lithos, v. 125, p. 825-835

Whipple, K.X., and Tucker, G.E., 1999, Dynamics of the stream-power river incision model; implications for height limits of mountain ranges, landscape response timescales, and research needs: Journal of Geophysical Research, v. 104, p. 17,661–17,674.

Whipple, K.X., 2001, Fluvial landscape response time: how plausible is steady-state denudation? American Journal of Science, vol. 301, p. 313.

Whipple, K.X., Wobus, C., Krosby, B., Kirby, E., Sheehan, D., 2007, New Tools for Quantitative Geomorphology: Extraction and Interpretation of Stream Profiles from Digital Topographic Data. Geological Society of America, Short Course: #506.

Willett, S. D., 1992, Dynamic and kinematic growth and change of a Coulomb wedge: In Thrust tectonics, p. 19-31, Springer Netherlands.

Wobus, C. W., Hodges, K. V., and Whipple, K. X., 2003, Has focused denudation sustained active thrusting at the Himalayan topographic front?: Geology, v. 31, p. 861-864.

Wobus, C., Heimsath, A., Whipple, K., and Hodges, K., 2005, Active out-of-sequence thrust faulting in the central Nepalese Himalaya: Nature, v. 434, p. 1008-1011.

Wobus, C., Whipple, K.X., Kirby, E., Snyder, N., Johnson, J., Spyropolou, K., Crosby, B., Sheehan, D., 2006, Tectonics from topography: procedures, promise, and pitfalls. Geological Society of America Special Paper, v. 398, p. 55–74.

Zonenshain, L. P., Kuz′min, M. I., Natapov, L. M., and Page, B. M., 1990, Geology of the USSR: a plate-tectonic synthesis: American Geophysical Union, v. 21, p. 1-242.